polygons in Figure 16 show the general area of each group of DSS wells included in the model. The ICAs in the model within each area are the grid cells containing wells.

In Figure 16 the information provided by the County about the DSS wells in the City of Cape Coral did not include all wells. However, a large amount of them are deep wells extracting from the Hawthorn Aquifer (outside the model domain).

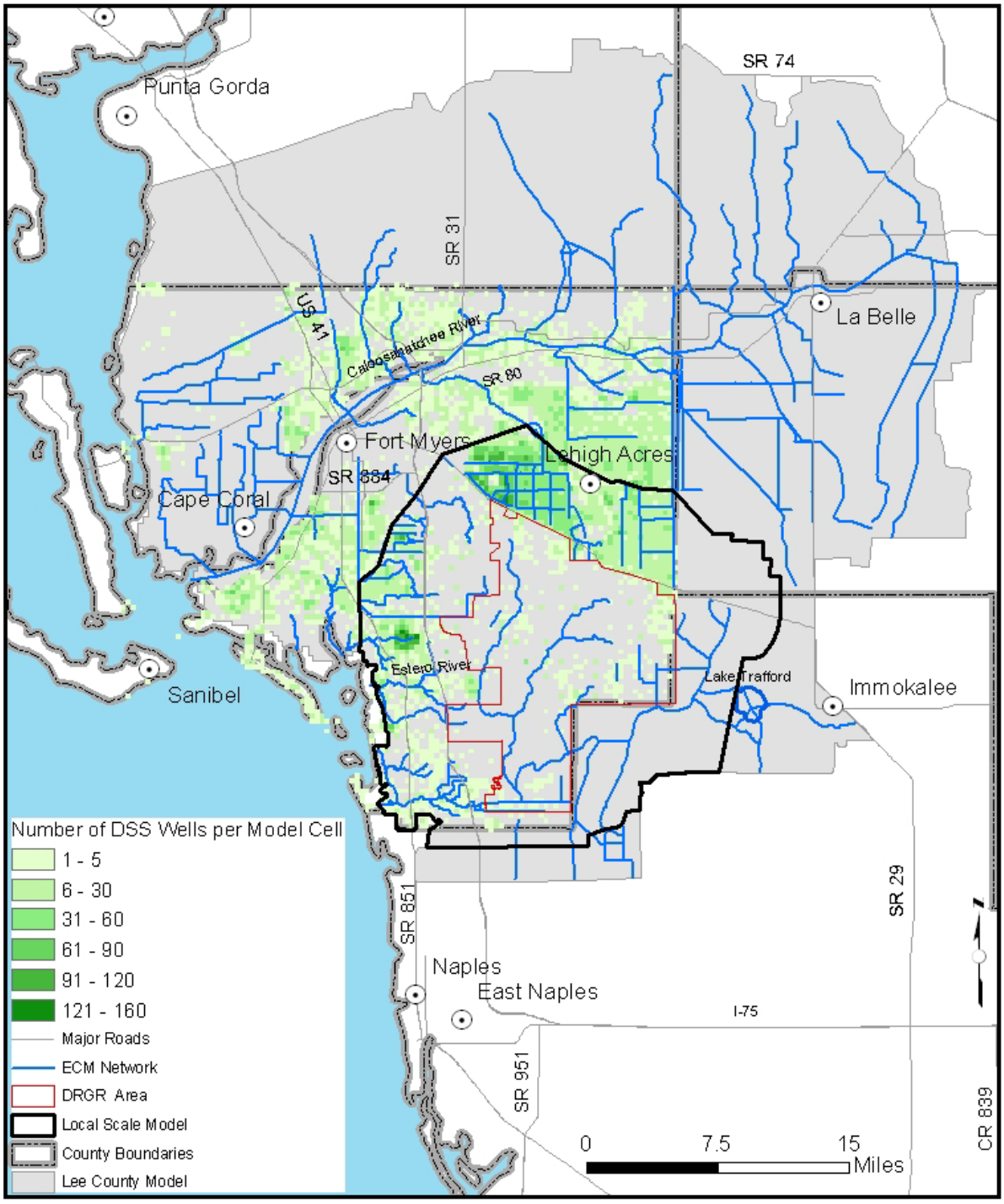

Figure 16. Domestic Self Supply Well Distribution.

A detailed description of the domestic self-supply ICAs defined in the model is provided in **Table 9**.

Table 9. Summary of ICAs defined to represent the water consumption from DSS wells.

ICA code	Total No. DSS wells	No. 1,500-ft cells	Include potable?	Well permitting region	Most used aquifer	Screen interval (ft)
545	58	3	Y	East Lee County	Sandstone	65 - 98
549	108	103	Y	Bonita Springs	Sandstone	65 - 98
551	7	15	Y	Bonita Springs	Lower Tamiami	65 - 98
557	98	1	Y	East Lee County	Sandstone	65 - 98
575	135	3	Y	East Lee County	Sandstone	65 - 98
579	160	213	N	Bonita Springs	Lower Tamiami	65 - 98
602	51	4	Y	East Lee County	Sandstone	80 - 130
606	89	33	Y	East Lee County	Sandstone	65 - 98
607	18	40	N	San Carlos/Estero	Sandstone	65 - 98
610	279	26	N	East Lee County	Sandstone	65 - 98
612	621	116	N	San Carlos/Estero and Bonita Springs (Coastline)	Lower Tamiami	65 - 98
626	69	39	N	San Carlos/Estero	Sandstone	65 - 98
1121	44	72	N	Fort Myers	Sandstone	65 - 98
1140	47	67	N	North Cape Coral	Lower Tamiami	30 - 65
1158	684	18	Y	North Fort Myers	Water Table	0 - 35
1159	286	127	N	Fort Myers and South Fort Myers	Sandstone	65 - 98
1164	3184	335	N	South Fort Myers	Sandstone	65 - 98
1166	479	22	N	Six Mile Cypress	Sandstone	65 - 98
1168	750	77	Y	Fort Myers	Sandstone	80 - 130
1171	1269	67	N	Six Mile Cypress	Sandstone	80 - 130
1172	2714	98	Y	San Carlos/Estero	Sandstone	80 - 130
1173	863	155	Y	North Fort Myers	Mid Hawthorne	160 – 230
1174	106	43	Y	Cape Coral	Mid Hawthorne	160 – 230
1175	15999	379	Y	Lehigh Acres	Sandstone	80 - 130
1178	1168	198	Y	East Fort Myers	Sandstone	80 - 130
1179	11455	674	Y	Lehigh Acres	Sandstone	80 - 130
1180	366	59	Y	North Fort Myers	Mid Hawthorne	160 - 230
1186	708	109	N	Cape Coral	Mid Hawthorne	160 - 230
1190	381	147	Y	Cape Coral	Mid Hawthorne	160 - 230
1193	1216	118	Y	Alva	Sandstone	80 - 130
1194	207	59	N	Cape Coral	Lower Tamiami	30 - 65

The following assumptions have been made in order to obtain an estimate of the average consumption of a domestic self-supply (DSS) well:

I. Maximum irrigation water demand is assumed to be 20 gallons per minute per pumping zone, 4 zones per house and each zone operated for 45 minutes per day. The total irrigation rate per house equals (20*45*4) = 3,600 gallons per house per day. Each house irrigates twice weekly; either Wednesday and Saturday, or Thursday and Sunday in accordance with Lee County regulations. Each house applies 75 percent of irrigation water between 12 am and 6 am; and 25 percent between 6 pm and midnight. The irrigation

pumping rate of one average well is then the average of the two possible schedules, which gives the application of the half rate, four times a week.

II. Potable water demand is assumed to be 100 gallons/per person/per day for uses like cooking, cleaning, and bathing with 3 people per household. The assumed consumption per capita per day is in the range from 100 to 130 reported by (Hammer and Hammer, 2001). The majority of usage (2/3) is assumed to occur in the morning between 6 am and noon while the remainder of usage (1/3) is assumed to occur in the evening between 6 pm and midnight.

Note that the maximum irrigation water demand is equal to or higher than the current irrigation consumption. The current consumption is in general higher during the dry season than during the wet season. The weekly time series for the maximum pumping rate of an average domestic self-supply well obtained from previous assumptions is presented in **Figure 17**. Two cases are considered corresponding to the use of DSS water for all the needs or just for irrigation in areas where the potable water demand is supplied from municipal wells. The weekly period in Figure 17 is then extended over the whole simulation period. The time series created has an average maximum pumping rate from a domestic self-supply well of 1029 gal/day (4.51×10^{-5} m^3/s) for irrigation only and of 1329 gal/day (5.82×10^{-5} m^3/s) including potable water consumption.

The maximum groundwater extraction rates for each ICA are found by multiplying the appropriate extraction time series (irrigation only or irrigation plus potable supply) for one averaged well by the total number of wells within the ICA. The extraction rate (or demand below this limit) is determined automatically by the model based on the soil moisture content.

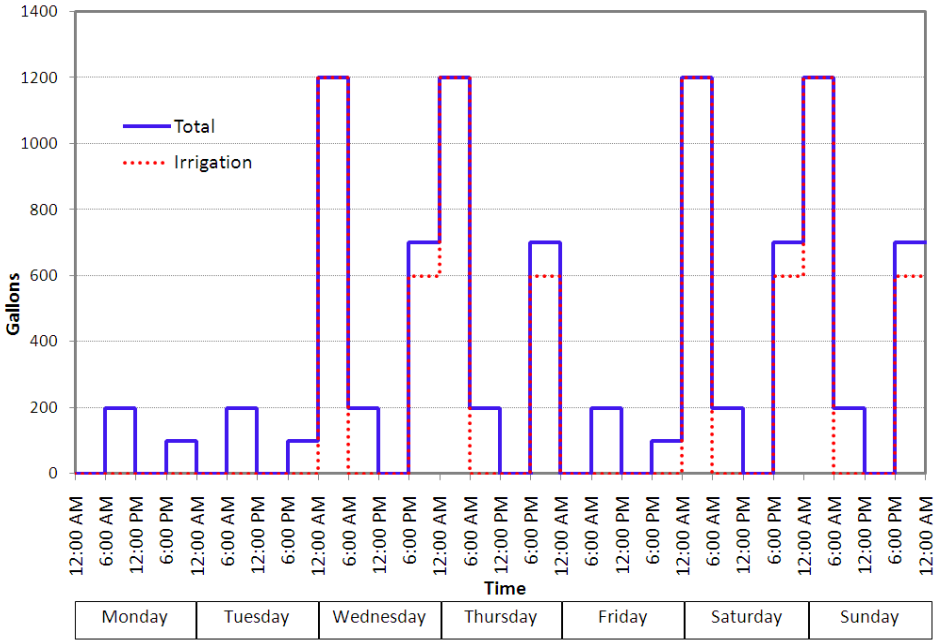

Figure 17. Maximum weekly consumption for a DSS well. The total volume includes irrigation and potable water supply.

Surface Water Model

Surface water is modeled in the overland component of MIKE SHE and in MIKE 11. The Overland Flow component solves the 2-dimensional diffusive wave approximation of the Saint Venant equations and MIKE 11 solves the fully dynamic Saint Venant equations in one dimension. The MIKE SHE overland component routes the surface runoff to the reaches defined in MIKE 11. MIKE SHE also has a drainage component that can route the drainage from urban or agricultural areas to the MIKE 11 canals.

ECM Development

MIKE 11 Model

The surface water model includes an extensive network of primary and secondary canals with many hydraulic structures, natural sloughs, rivers, and lakes. The surface water network is modeled using DHI's one-dimensional hydraulic model, MIKE 11. Inputs for the MIKE 11 model consist of the river network path, channel cross-sections, boundary conditions, and bed resistance. Moreover, structures such as culverts, dams, bridges and control gates that may alter river flows and stages are specified as input to the model. The ECM MIKE 11 network and structures is shown in **Figure 18**.

The network was built using the SWFFS canal network as the starting point and adding secondary canals and structures from the EIC, BCB and TCRB sub-regional models to build the BLM. In addition, secondary canals and structures were added or updated from the

ECWCD model. Finally, the structures in Alico and Corkscrew roads were also updated or included based on the information received from Lee County.

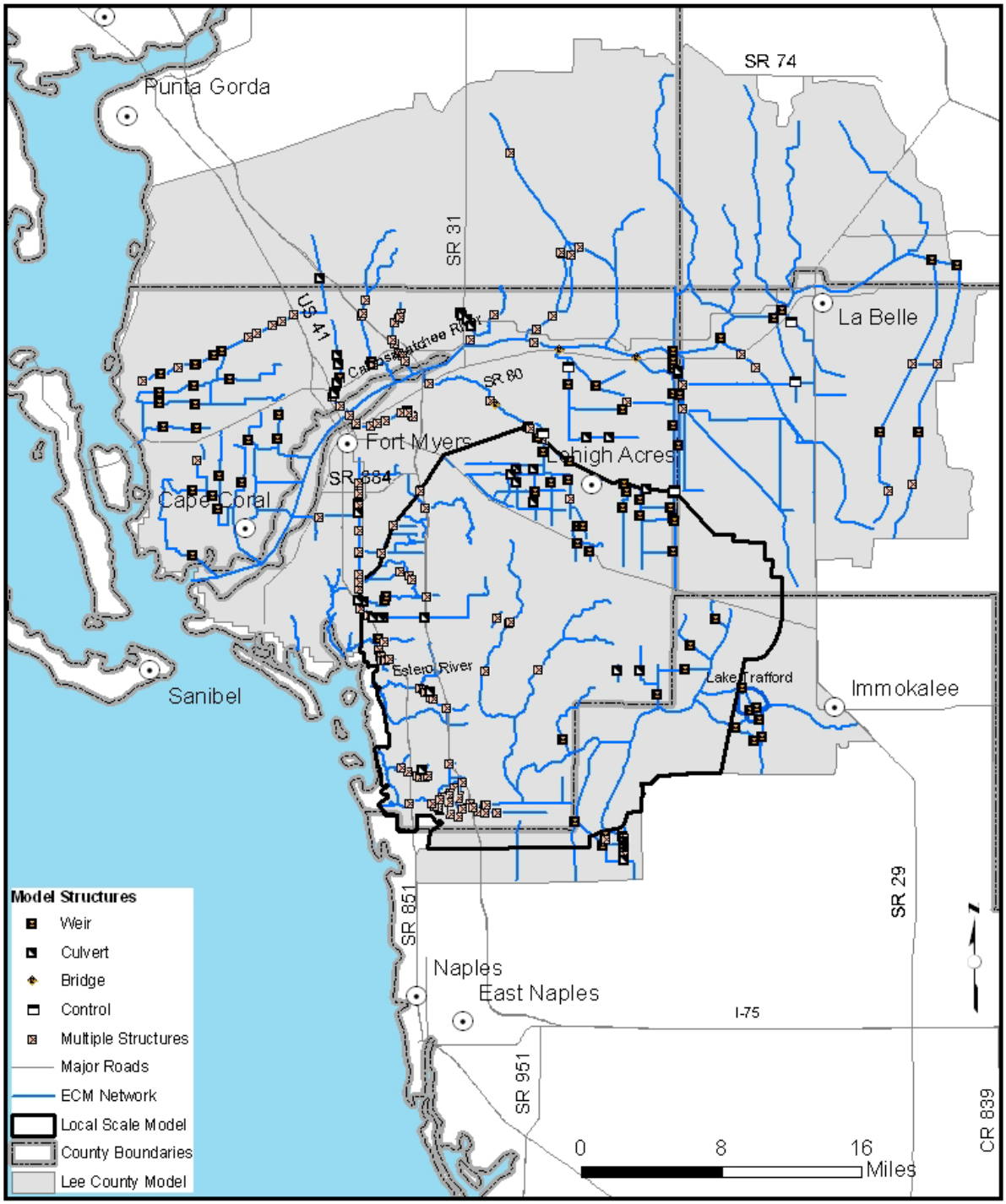

Figure 18. MIKE 11 Network and Structures in the ECM.

MIKE SHE and MIKE 11 Interaction

Water flow is exchanged dynamically between the MIKE 11 hydraulic model and the MIKE SHE hydrologic model. The MIKE 11 canals exchange water with the underlying aquifer, driven by the head gradient and controlled by either the aquifer conductivities or by a river lining leakage coefficient, or a combination of both. Runoff from the MIKE SHE overland surface is driven by topographic gradient and flows into MIKE 11 in places where both the river bank elevations and the water levels are lower than the water elevations in adjacent MIKE SHE cells. MIKE 11 branches also receive water from the drainage component of MIKE SHE.

Flooding from the MIKE 11 rivers, lakes or canals to the overland surface in MIKE SHE is allowed to occur where specified. The flooding method used for the ECM is the flood code mapping option. This method is appropriate for modeling lakes, wide rivers and sloughs. The flood code approach ensures that the volume of water is not double counted in the same spatial location that the branches and the flooded MIKE SHE cells occupy if the extents of the specified flood coded cells are consistent with the cross section widths of the MIKE 11 branches. **Figure 19** shows the flood code map used for the ECM. The flood coded cells are the MIKE SHE cells where the water from MIKE 11 canals is allowed to spill out. The movement of water in flood coded cells along the river direction is controlled by MIKE 11, but this water is also available for all other MIKE SHE processes, such as evaporation, overland flow, and infiltration.

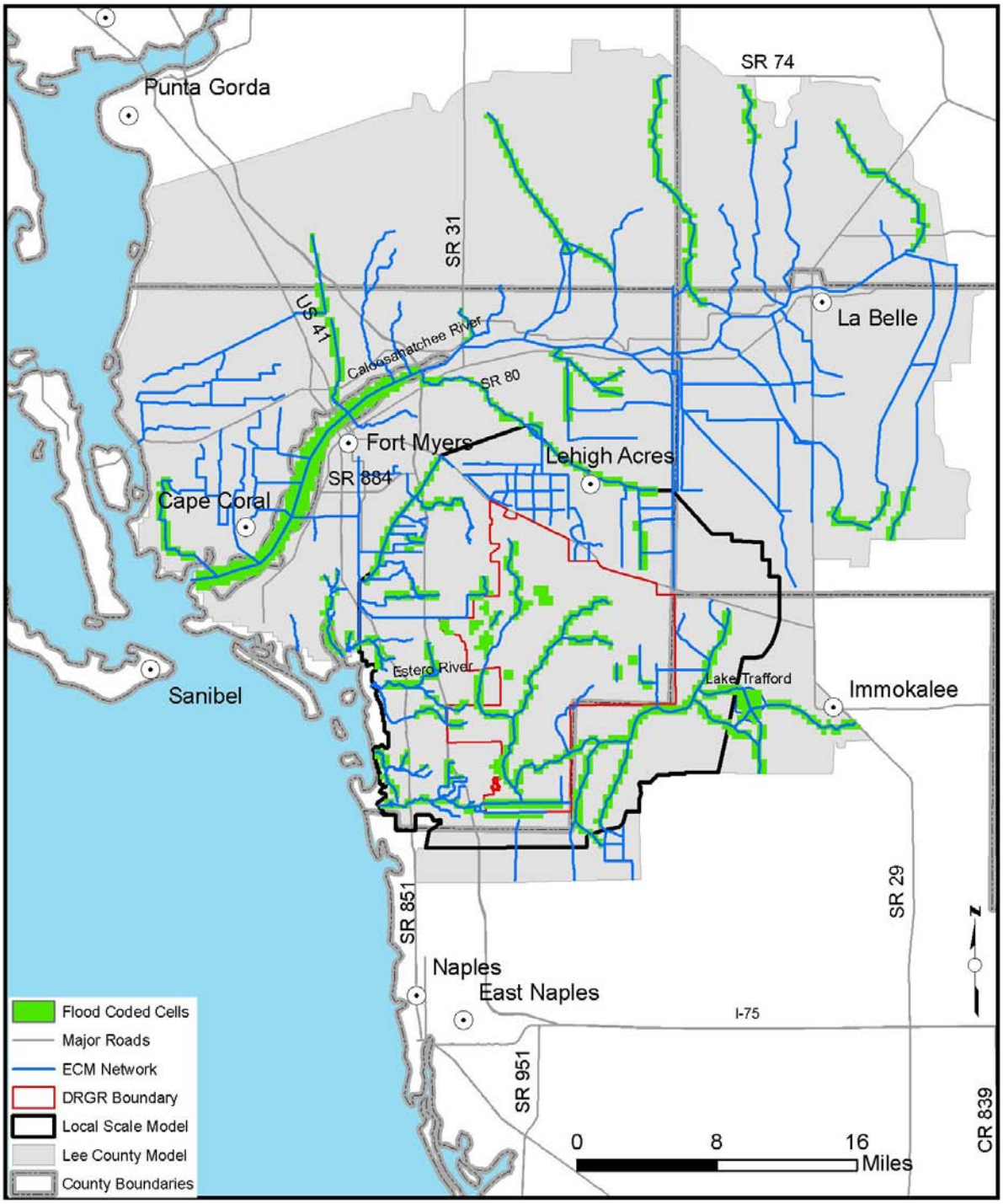

Figure 19. Flood coded cells in the ECM.

Representation of Roads and Berms

Due to the relatively large size of the model cell size (1,500 feet), the elevations of certain features that impede flow between certain areas are not properly represented in the model topography. The separated flow areas are specified in the overland flow module in MIKE SHE to define localized higher topography that would prevent overland flow from naturally occurring from one area to another. For example, an elevated roadway would prevent overland flow except at designated culvert crossings. Another example would include a farm field or mining operation that is bermed on all sides to prevent overland flow from surrounding areas.

Discussions with Lee County staff revealed that Alico and Corkscrew Roads serve as barriers to natural overland flow. Multiple culvert crossings exist along the right-of-ways to allow flow to move towards the south and towards the west. The existing separated overland flow areas defined in the SWFFS model were further subdivided to account for the barriers defined by Alico and Corkscrew Roads. Moreover, additional branches and structures were defined in the MIKE 11 river network to represent the culvert road crossings under these roadways, as stated the previous sections.

Separated flow areas were also defined for the mining pits to represent the surrounding berms. This approach assumes that there is no overland flow between the mine and surrounding properties. In some agricultural or urban areas in the DR/GR Area, separated flow areas were also defined. The separate flow areas map used for the ECM is shown in **Figure 20**.

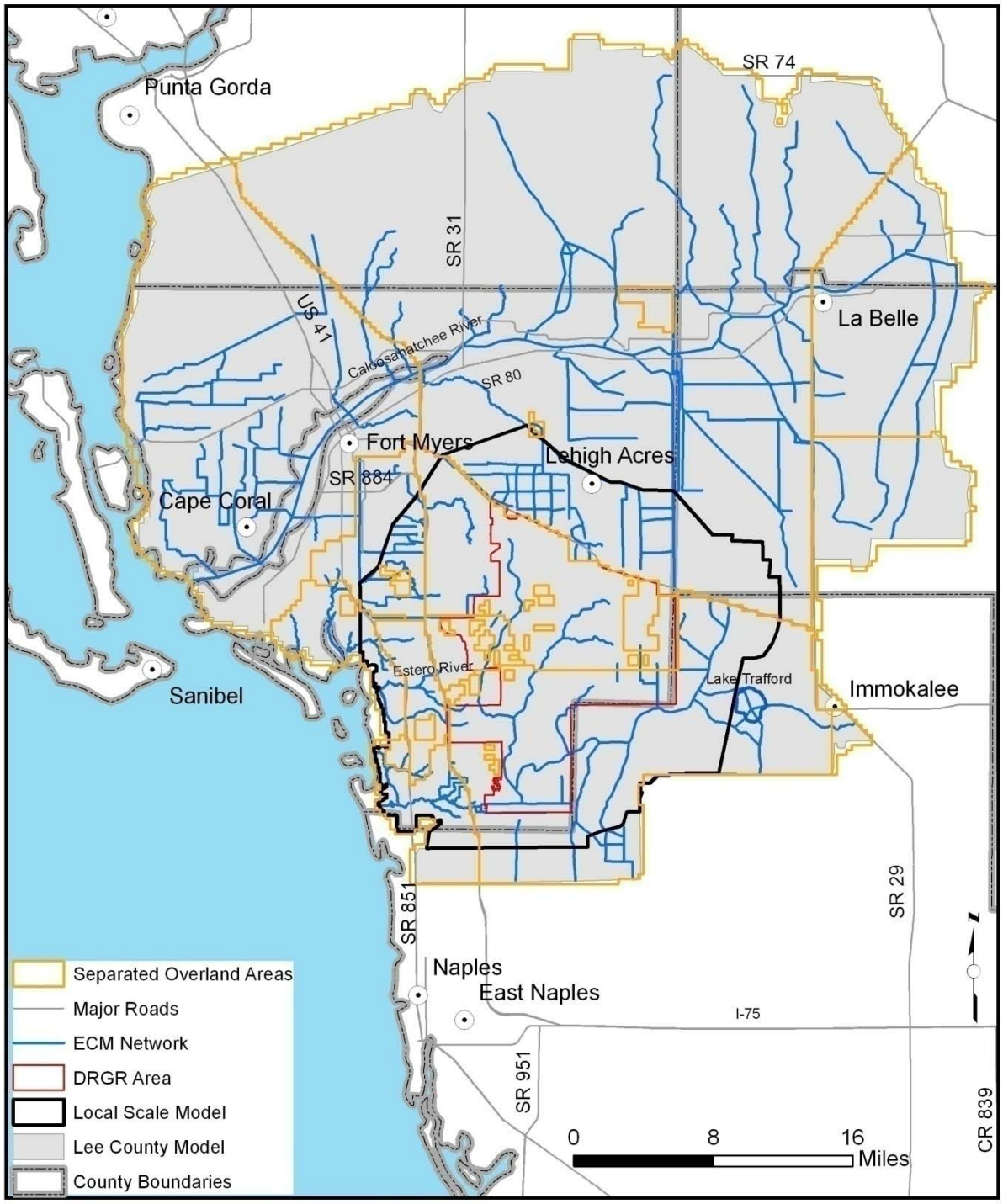

Figure 20. Separated Overland Flow Areas in the ECM.

Representation of Mining Pits

There are several mining pits in and around the DR/GR Area that may alter the water budget in the region. Those mining pits are open water bodies that may have higher ET rates than the pre-developed land. In open water conditions, there is more storage (porosity) than in pre-existing soils, and the amplitude of the changes in the water table level are lower than in subsurface pore water at equal volumetric fluxes from rainfall, ET, infiltration, etc. Moreover, open water bodies represent high hydraulic conductivity areas that flatten the preexisting regional hydraulic gradient and drain upgradient pore water.

The representation of the mining areas includes the following:

1) The Environmental Resource Permits (ERPs) for mines require that at least the 25-year three-day (or, in some cases, the 100-year) storm events are contained. In order to represent the berms, a separate flow area was defined at the boundaries of the mining pit areas. The separate flow areas prevent overland flow to or from surrounding areas. The separate flow areas corresponding to mining pits in the ECM are shown in Figure 20.

2) Dover, Kohl and Partners provided the depth of the mining pits in and around the DR/GR Area from official records. This information was used to assign the bottom elevation of the conceptual mining pit lens at each corresponding grid cell in the model. This approach, which has been used in other groundwater models (May-Chu and Freyberg, 2008), allows lateral exchange from the mining pit to the adjacent groundwater cells. The mining pit lens is set with a high conductivity (K_h= K_v= 1 m/s = 2.8×10^5 ft/day) and the maximum specific yield (Sy= 1), to mimic open water conditions. Some of the deeper mining pits reach the upper part of the Upper Peace River Confining Unit, which is the third computational layer of the model.

3) A portion of the mining pits were etched in the model topography to ensure that there is ponded water through the simulation. The portion of the mining pit below the level burned in the topography is represented in the groundwater model as a geological lens.

4) After converting the higher resolution land use maps to the model resolution, the maps were modified to ensure that all mining pits were defined using the same code equal to "water". This allows the proper application of land use based parameters for these areas, such as ET parameters to calculate the proper evaporation rate from open water.

Surface Water Boundaries

Measured water levels and flows were used to define the surface water boundary conditions for the ECM. The surface water time-varying boundaries are shown in **Figure 21**. In MIKE 11, boundary conditions are required at the unconnected ends of all branches. The unlabeled unconnected ends in Figure 21 are set as zero-flux (or closed) boundaries. The eastern boundary of the canal network is located at the S-78 structure in C-43 Canal. The measured discharge at the S-78 structure was specified for this location from DBHYDRO.

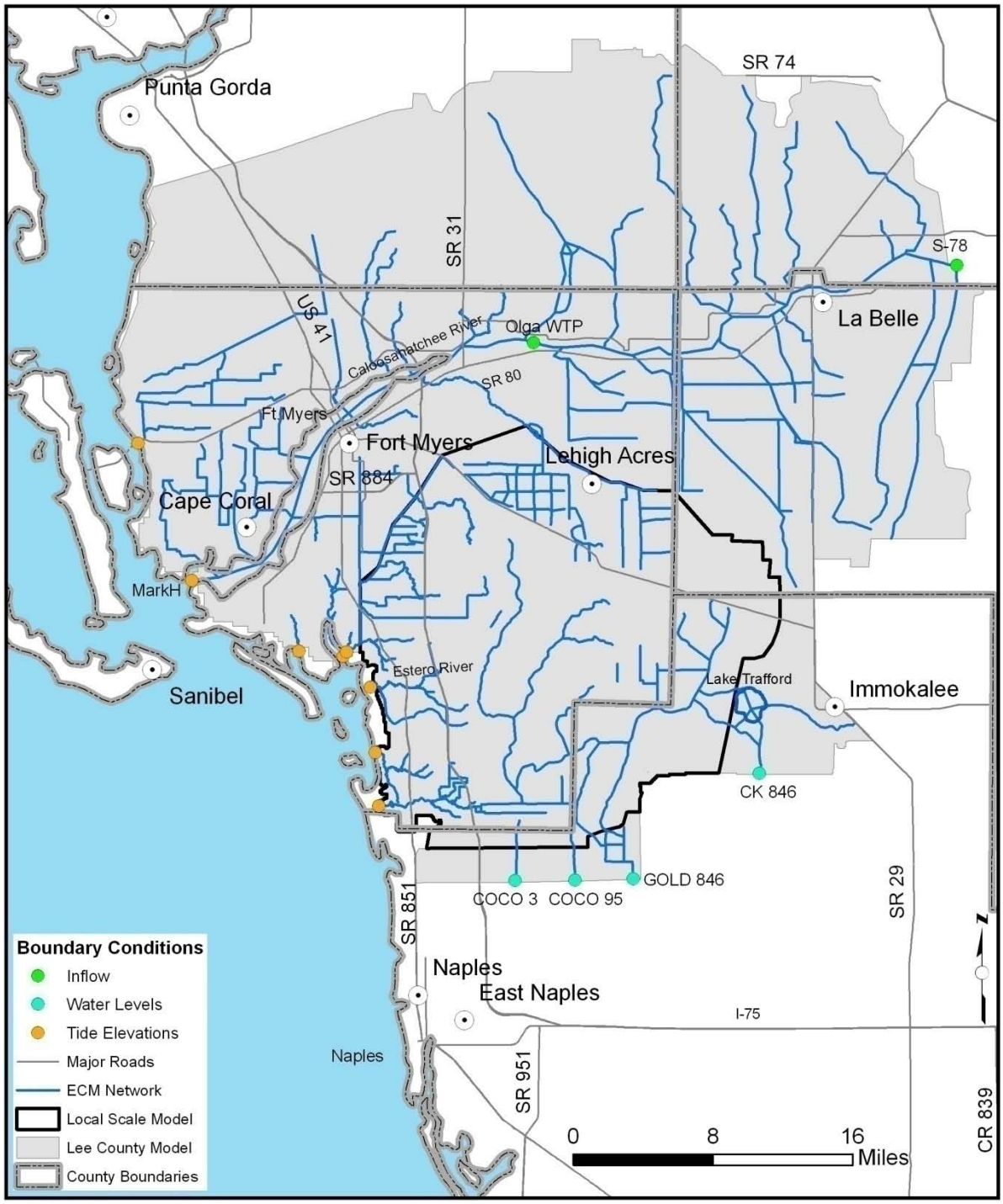

Figure 21. MIKE 11 Time-Varying Boundary Conditions in the ECM.

The south-eastern boundaries consist of the Camp Keais Strand at the CR846 crossing and Immokalee Canal at the intersection with SR29. The available stage data from DBHYDRO for the Camp Keais Strand at the CR846 crossing was applied at this location. A closed (no-flow) boundary was specified for the Immokalee Canal.

The ECM area was extended from its original proposed area in order to reduce boundary effects in the southern part of the DR/GR Area. The new southern surface water boundaries consist of the set of downstream ends of canals that drain to the Cocohatchee Canal. The water level time series from Cocohatchee stations were used as the boundary conditions specified at the southern end of these canals.

The Olga Water Treatment Plant (WTP) at Fort Myers was included as a point source intake from the river network, as in the SWFFS model. The original time series data was updated, with the daily data delivered by Howard S. Wegis, at Lee County Utilities, from April 2001 to December 2007.

The hourly tidal water levels from the NOAA (http://tidesandcurrents.noaa.gov/index.shtml) Naples station were used for all the west coast boundaries. This station was determined the most suitable tidal station for the western area of the model after a comparison was performed between the available tidal data. The two NOAA stations within or close to the model area that have data available for the entire simulation period are: the Fort Myers station (ID: 8725520), which is approximately 13 miles upstream from the coastline at the Caloosahatchee River, and the Naples station (ID: 8725110), which is approximately 10 miles south of the southern boundary of the model domain (see **Figure 22**). The MARKH station from DBHYDRO, located at the downstream end of the Caloosahatchee River, does not have data available for the entire model simulation period. The average hourly and daily data from the Naples and Fort Myers stations were compared to the daily average data from the MARKH station. The recorded values at this station appear to slightly overestimate the daily averages of the other two stations. There are also some differences between the Fort Myers and Naples stations. First, the oscillations of the hourly time series differ in amplitude and phase. Second, the daily averaged elevation at Fort Myers station is slightly higher in general than at the Naples station. These differences are to be expected since the Fort Myers station is farther upstream from the coastline. Thus, it was determined that the Naples station is more representative of the coastal water levels.

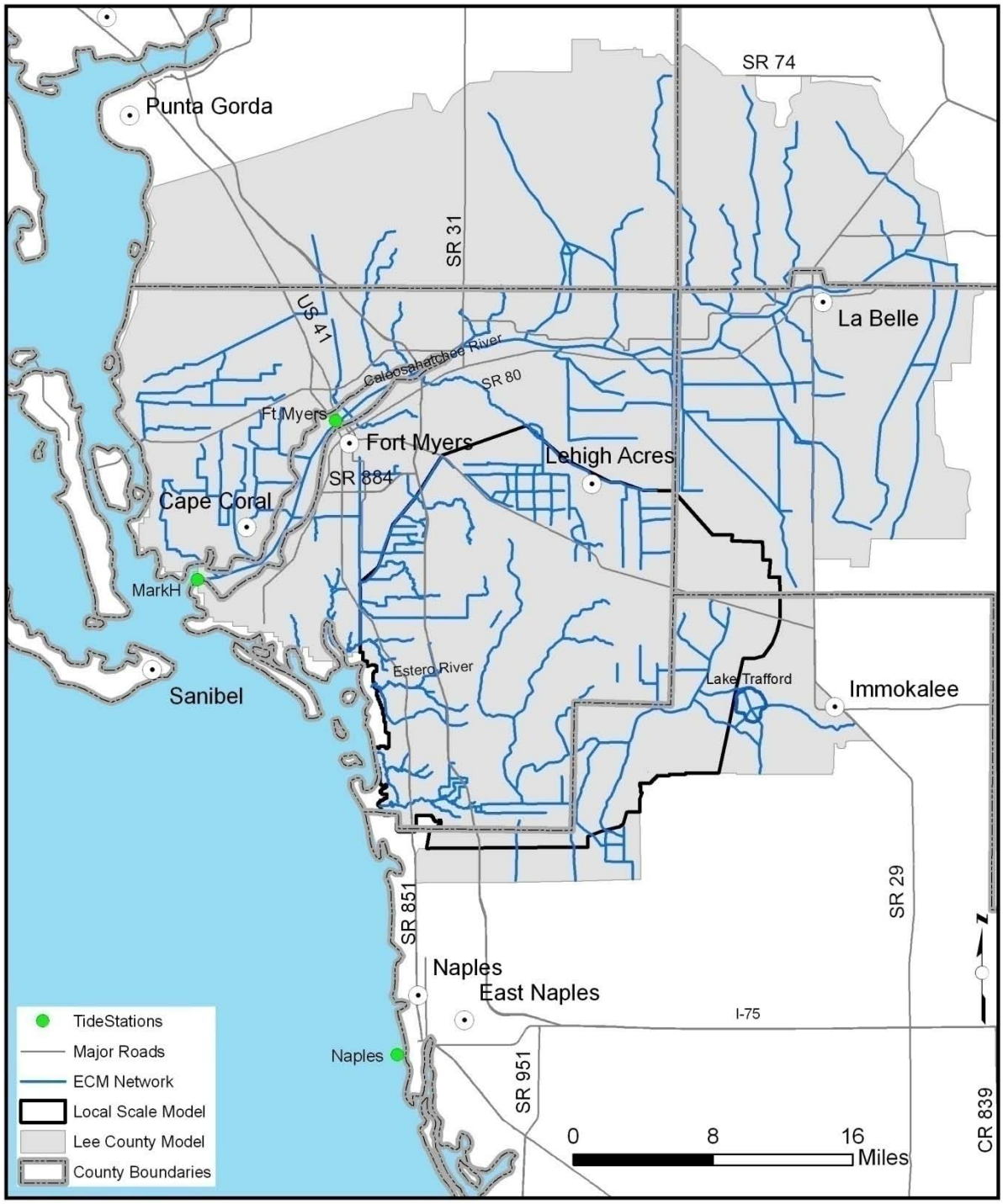

Figure 22. Tidal Stations.

LS ECM Development

Several refinements were made to the surface water component of the LS ECM. Some of the refinements are described below.

- The mining pit coverage was redrawn at 750-ft resolution maps (down from 1500 ft resolution in the ECM) for conceptual lens depth and separated overland flow areas. The separated flow area map with higher resolution was also improved to better represent the road divisions. The drain code map used in the LS ECM was obtained in a similar way as in the ECM from the separated overland flow areas map by setting zero drain codes at mining pits and allowing drainage to the boundaries.
- The 750-ft land use map contains other grid cells classified as water that are not considered as mining pits in the model. Aerial photos reveal in most of those cells well defined open water bodies with sizes from one to several 750-ft grid cells. Those cells are referred to as "shallow lakes" and they were conceptualized in a similar way as mining pit cells. For shallow lakes where the depth was not provided by Dover, Kohl and Partners, a value of 10 ft was assumed.
- The distribution of mining pits and shallow lakes in the LS ECM domain area is shown on **Figure 23**. The representation of the water bodies can be revised in the future, when more information becomes available about the interaction of the water body with the surrounding cells (i.e. presence of berms, drainage system, etc). Also, information about the bathymetry of the water bodies can improve the representation in the model.
- Another improvement in the LS ECM is the representation of contiguous water bodies that are divided by land areas narrower than one grid cell size, like roads for example. As with the ECM, separated overland flow areas were established to prevent communication in the overland component. For the LS ECM, the sheet piling module in the groundwater component was added to the model. Since the separation between the water bodies was less than one grid cell, the model would have shown these water bodies as touching each other without any hydrologic barrier between them. The sheet piling allows for the specification of a hydrologic barrier between these touching water bodies that more closely represents reality. Since mining pits and shallow lakes are represented with a groundwater lens, free communication between contiguous water bodies through the groundwater layer is prevented by introducing conductivity barriers, i.e., artificial sheet pilings. The locations of the flow barriers were found by inspecting aerial photos and assuming the lack of culverts on those divisions. The divisions are shown in Figure 23. A uniform leakage coefficient of 10^{-4} sec^{-1} was assumed by considering divisions of 50 ft wide and a typical conductivity of the Holocene-Pliocene geological layer.

  Other improvements and refinements to the surface water system in the LS ECM are described in the following sub-sections.

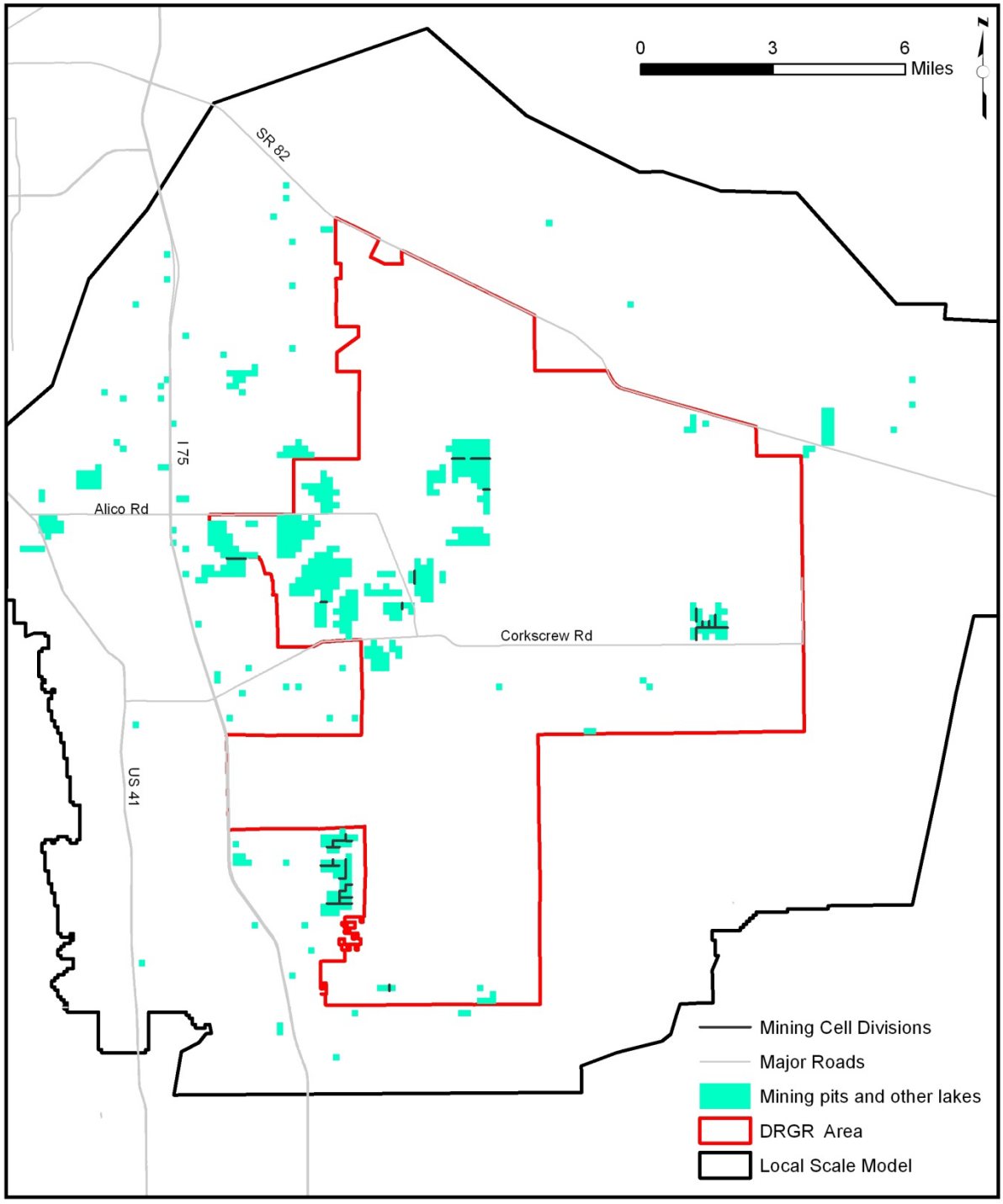

Figure 23. Mining Pits and Shallow Lakes.

Definition of Flow Ways

The inclusion of all the main flow ways in the MIKE 11 component of the model has advantages over using a combination that alternates channel flow and overland flow. MIKE 11 solves the surface water (channelized) flow problem in a more accurate way since it solves the exact equations in smaller time steps and accounts for the channel geometry (or micro-topography). On the other hand, the overland flow component considers two dimensional flow, which is beneficial for wide flow ways (sloughs, lakes, etc) where the flow across the main path (e.g., toward the center of the slough) may be important. The approach followed by DHI to represent the sloughs and lakes in this model is to create a MIKE 11 branch for the slough center flow with a 750-ft wide cross-section and allocate a flood code to allow full interaction with the overland component that controls the 2D surface water flow in the neighboring areas.

The definition of new MIKE 11 branches containing the main flow ways was conducted based on the following information:

1. The 5-ft resolution LIDAR topographic map. In this map, the highs (berms and roads) and lows (canals, creeks and sloughs) are clearly visible. Some bridges are removed from flow ways. However, the existence of some culverts is sometimes difficult to determine from this map.

2. Hydroperiod map from KLECE. Natural flow ways like sloughs are likely present in connected natural areas. High and low hydro-periods are useful to delineate flow path ways in some natural areas.

3. Aerial photos from 2007 (and 2004 outside of the DR/GR). They were useful to delineate pathways particularly where there is not LIDAR topographic data.

4. Notes received from Kevin Hill (dated from 5/27/2008). They were useful to delineate flow ways along and across Corkscrew Road.

5. GIS processing of topographic data. The new LIDAR topographic data was averaged to 100 ft resolution and merged into 100-ft SFWMD data from 2004 in order to “fill the gaps” outside the Lee County areas. The resulting 100-ft resolution topographic file was processed in ArcMap to obtain the flow ways. A similar processing was conducted to a 750-ft resolution topographic map obtained from those two topographic data. The flow path ways obtained in both cases cannot be used directly as the existing flow ways (mainly because of the lower resolution that blur canals and creeks and because this processing does not include the culvert information), but they serve as a guide for the more detailed flow ways delineation conducted visually from the previous information.

The flow ways analysis described above led to a drainage network that was too detailed. That network was later reduced to the coarser MIKE 11 network used in the model.

Figure 24, **Figure 25** and **Figure 26** show the network structures, the flood coded cells and the separate overland areas considered in the new model in conjunction with the new flow ways definition.

ADA Engineering, Inc. [2008] performed some work on the MIKE 11 network in the area between the Estero and Imperial Rivers based on local survey information. The MIKE 11 network of this model was based in part on the MIKE 11 network generated by ADA Engineering, Inc.

While building the MIKE 11 network, considerable effort was made to ensure that all important flow ways were included. However, the network may include flow ways that conduct minimal flow since it is difficult to predict the relevance of all the flow ways considered. Once the network is introduced in the model, the flow rate predicted by the model would allow us to evaluate the importance of each flow way.

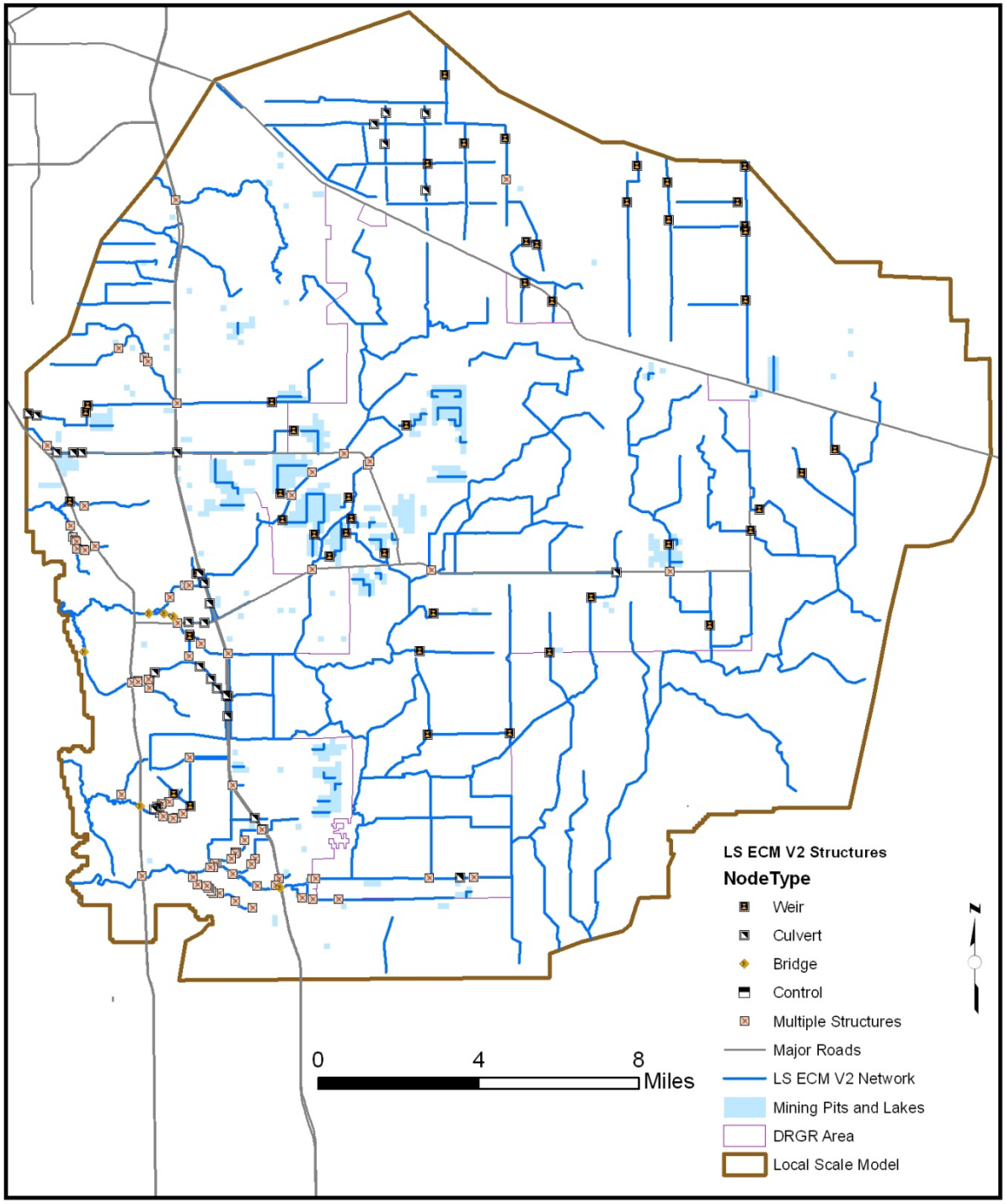

Figure 24. MIKE 11 Network and Structures in the LS ECM.

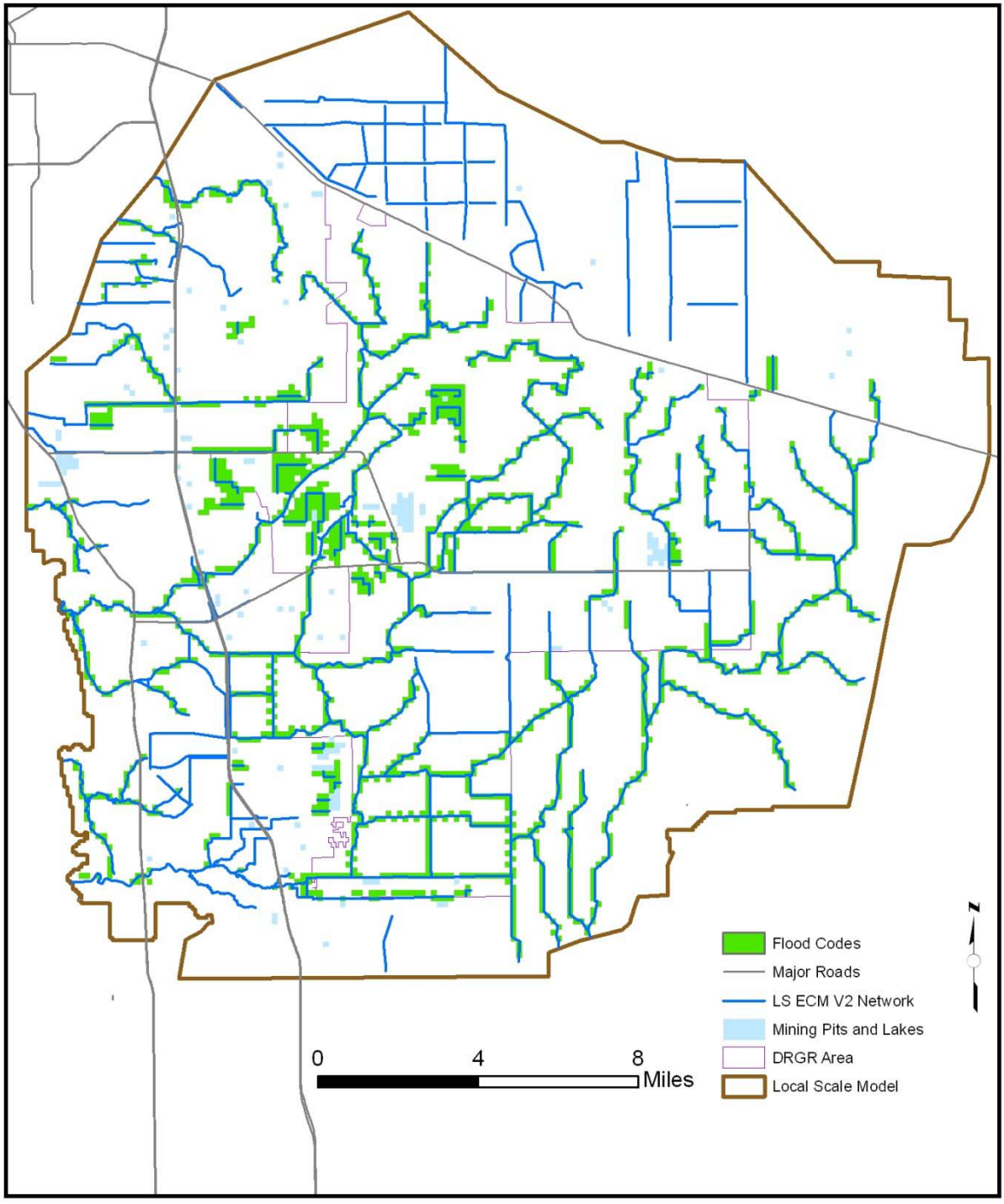

Figure 25. Flood Codes in the LS ECM.

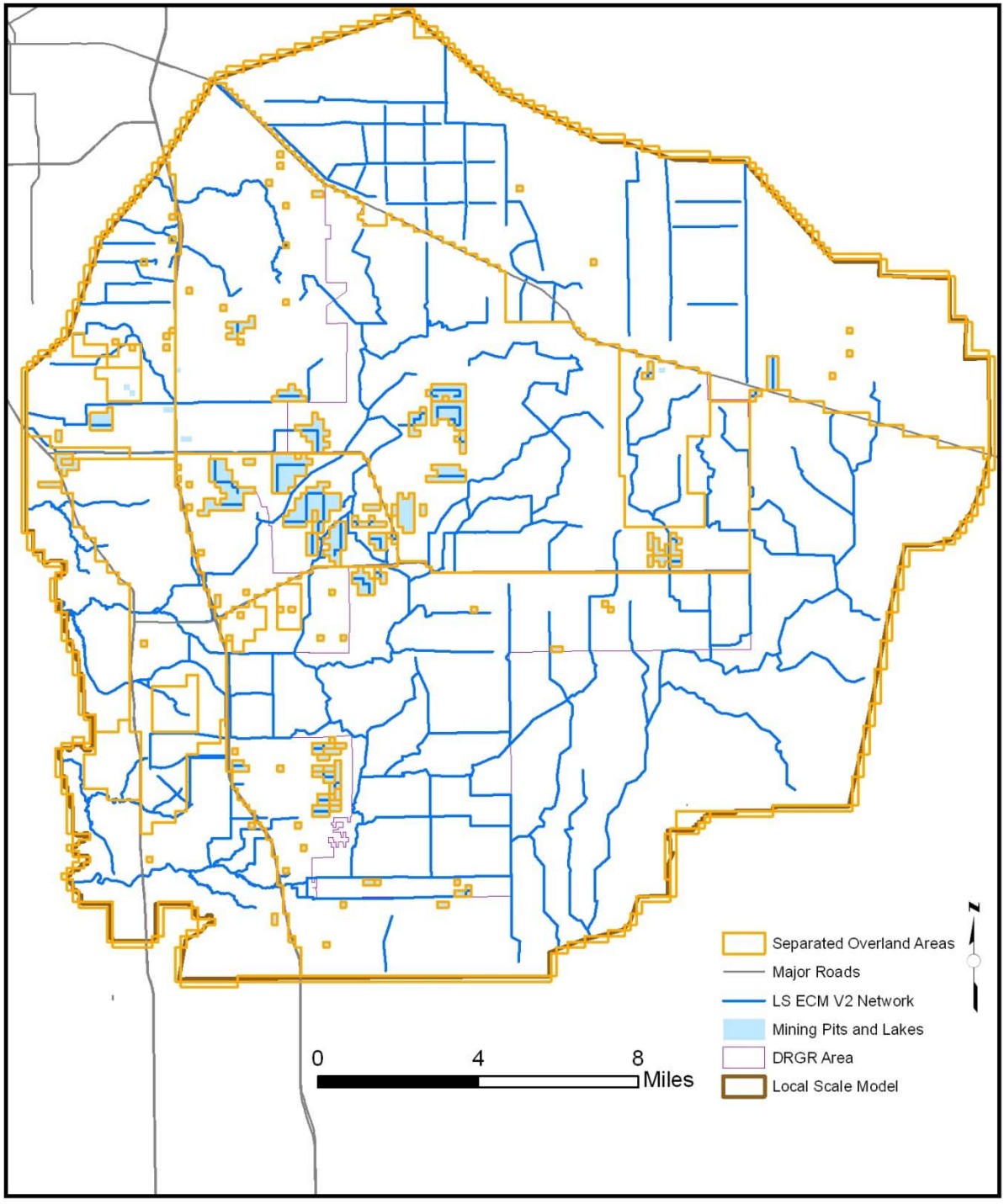

Figure 26. Separated Overland Flow Areas in the LS ECM.

Cross-section Extraction

The cross-section geometry for the MIKE 11 branches was extracted by using the MIKE 11 GIS tool. The 5-ft resolution topographic map was used where available and the SFWMD 100-ft resolution map otherwise. Cross sections were spaced a distance of about two grid cells (~1500 ft). It is recommended to have as many cross-sections as possible to assure a better representation of the channel geometry, but cross-sections spaced less than one grid cell apart may produce instabilities in the model.

In some cases, water in the channel prevented the LIDAR from reaching the channel (or cross-section) bottom. Thus, the cross-sectional geometry of the submerged part was taken from previous surveyed cross-section data. Unfortunately, the LIDAR data was acquired between the months of June and October of 2007 and not at the end of the dry season when the water levels are lower and the bottom of most of the flow ways are dry, which would allow a better estimation of the cross-section geometry from the LIDAR data.

Drainage around Mining Pits

The initial assumption of bermed mining pits used for the ECM is not always the case as revealed following a visual inspection of the high resolution LIDAR topographic map available for the LS ECM development. The fact that some mining pits may be collecting or releasing water from the nearby areas may be relevant to better account for water levels in the mining pits and the discharge rate of nearby flow ways.

The drainage system conceptualized in the MIKE 11 component around some of the mining pits is shown in **Figure 27**. In cases where the mining pit is not fully bermed, a MIKE 11 branch was included to connect the branch that accounts for the standing water at the mining pit and a nearby flow way. A conceptual weir structure is also included in the connecting branch to provide better control of the elevation above which discharge to or from the mining pit occurs.

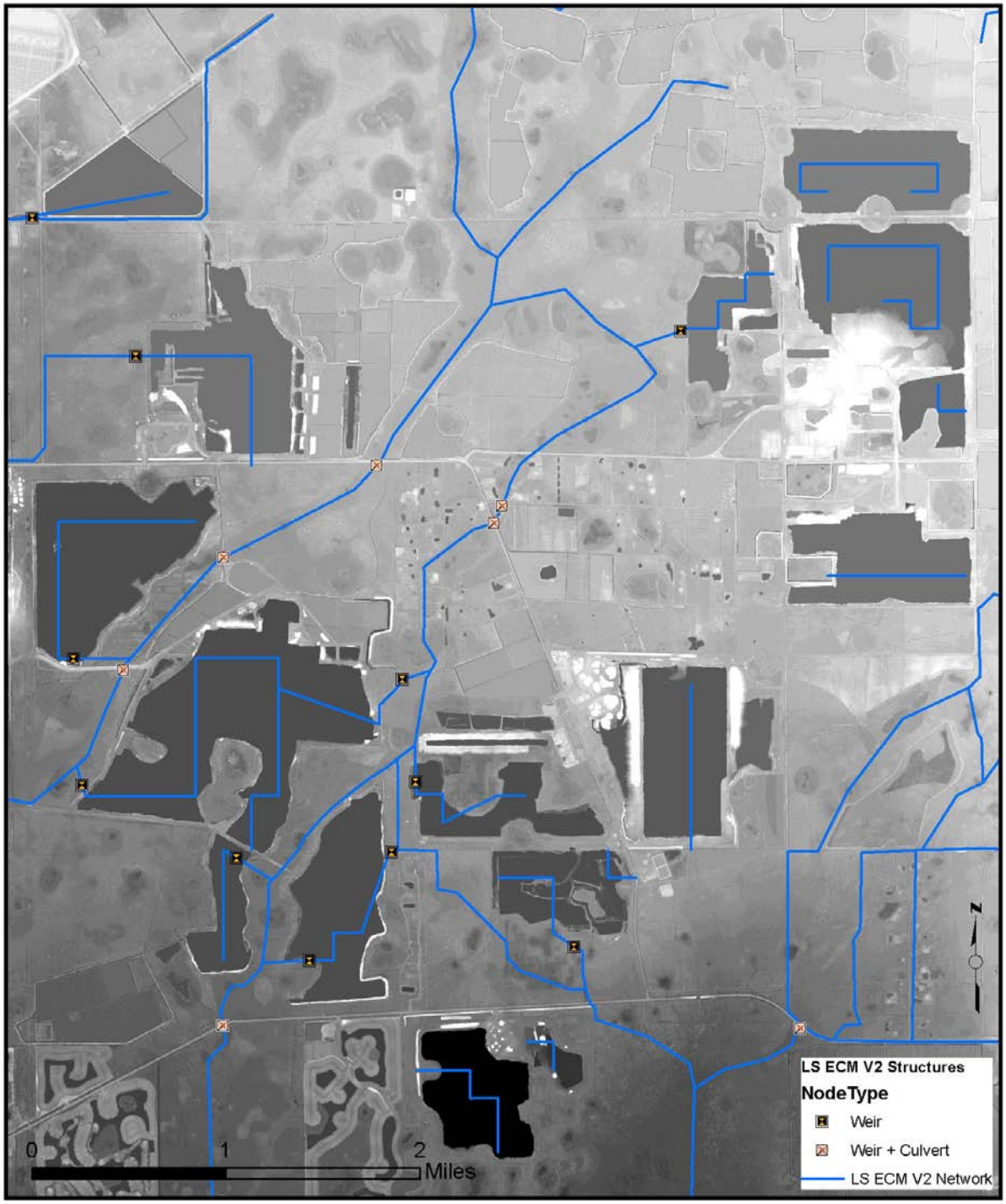

Figure 27. Drainage system around mining pits with a grayscale shaded relief map of LIDAR topographic data in the background.

Note: Lighter areas in the topographic map represent higher elevations, darker represent lower-lying areas.

Model Calibration

Calibration of the ECM and LS ECM was performed for the period of January 1st, 2002 to November 1st, 2007. As part of the model development, considerable effort was spent to improve the representation of certain important features in the model, such as the mining pits and flow ways in the DR/GR Area. Furthermore, a number of model parameters, such as overland flow roughness coefficients, hydraulic conductivities and storage parameters of the geological layers, and subsurface drainage parameters, were tested and varied in order to produce a closer match between model results and observed data. The observation time series data consist of stage and flow time series from surface water stations and of water table levels from observation wells. The surface water data was obtained from DBHYDRO and the groundwater data was obtained from Lee County, DBHYDRO, and the USGS. These data were used to compare the model stages, flows, and groundwater heads at the corresponding locations. For the Lee County Model Area there are a total of 143 groundwater monitoring wells, 31 surface water stage and 10 surface flow stations. Due to the time limitations of this project, DHI and Lee County agreed to focus the calibration of the model on the following areas, listed from highest to lowest priority:

1. The DR/GR Area and the Imperial River Basin.
2. The Orange River basin in the area south of Able Canal.
3. The Six Mile Creek Basin in the area west of the DR/GR.
4. The areas north of Caloosahatchee River and east of the S-79 structure in the freshwater Caloosahatchee River basin.

The calibration was focused primarily on the ECM. However, after extracting the higher resolution model (LS ECM), some additional calibration and improvement efforts continued in both models simultaneously.

After including the changes in the LS ECM derived from the new topographic data, some instability appeared in the MIKE 11 network. Instabilities increase the water balance error and may affect the accuracy of the model results. Moreover, further adjustments were required in the model in order to improve performance at stations where performance had decreased. Thus, a limited-time recalibration was conducted for the LS ECM following the update with the high resolution topographic data.

Model Improvements

As part of the model development, considerable effort was spent to improve the representation of certain important features in the model, such as the mining pits and flow ways in the DR/GR Area. Furthermore, a number of model parameters, such as overland flow roughness coefficients, hydraulic conductivities and storage parameters of the geological layers, and subsurface drainage parameters, were tested and varied in order to produce a closer match between model results to observed data.

ECM

The overall performance of the model was improved by focusing primarily on the DR/GR Area. The most relevant changes in the ECM are summarized below.

1) Some cross-sections and structures in the river network were corrected according to previous sub-regional models. Several cross-section shapes were also modified to meet structure geometry and in other cases to follow the topography. The cross-section widths of flooding branches were adjusted to match the MIKE SHE flood codes. The Manning's roughness coefficients and the leakage coefficient were modified in some of the MIKE 11 branches.

2) The original overland Manning's M (1/n) global values were modified for Hydric Flatwood (3.33 to 4.0), Marsh (1.67 to 2.33) and Cypress (2.5 to 3.33).

3) Additional separated overland flow areas were added to represent flood control features around some agricultural areas in the DR/GR Area. The overland boundary conditions were adjusted in MIKE SHE to represent time-varying conditions.

4) Drain depths and time constants for agricultural areas were decreased to 0.5 ft and 0.25 day^{-1}, respectively; in order to improve the model performance around the DR/GR Area. The drain code map was adjusted to match the separated overland flow areas map in relevant areas. Drainage was set to zero in mining pits. Drain flow was allowed to flow from agricultural and urban areas to the model boundaries.

5) The screen interval and maximum pumping rate in some ICAs were modified based on previous sub-regional models.

6) Mining pits were conceptualized as described in a previous section.

7) The hydraulic conductivities of the different geological layers and lenses were adjusted during the model refinement process. The conductivities for the different geological layers and lenses were taken initially from the SWFFS model. In this model, the conductivity values were recognized as having high uncertainty and they were considered as calibration parameters (CDM, 2006). During an inspection of the resulting conductivity maps, it was found that there were areas with high vertical conductivities in relation to the horizontal conductivities, which may have resulted from these parameters being calibrated independently. In the ECM, the vertical conductivity for the Water Table Aquifer was limited to a value equal to, or lower than the corresponding horizontal conductivity. Also, conductivities of the two confining lenses and the Sandstone Aquifer were considered isotropic. The isotropy assumption is reasonable because in the model the computational layers 2 and 3 are each composed by one lens and one geological layer (Figure 12). The confining units (represented as lenses) are less permeable than the aquifers (represented as geological

layers). Thus, the conductivity of the lens defines mostly the vertical conductivity of the computational layer and the geological layer conductivity defines the horizontal conductivity. The final conductivity maps obtained after the refining process are illustrated in Appendix A.

8) The specific yield in the upper geological layer was changed from 0.2 in most areas to a uniform value of 0.15, as suggested by SFWMD. The results of the model show no significant variation in response to this change.

9) The storage coefficient in the three aquifer layers was changed from a distribution with a mean value of approximately $4*10^{-4}$ ft^{-1} to a uniform value of 10^{-4} ft^{-1}. Seasonal fluctuations in the groundwater head in deep layers were slightly increased by decreasing this coefficient. The storage coefficient in the model could be decreased further to improve the performance of the model in deeper layers. The minimum possible value of the storage coefficient occurs with negligible porous matrix compressibility. Considering the water compressibility is equal to $5.3*10^{-5}$ atm^{-1} and the porosity is equal to 0.2, the minimum possible storage coefficient value is estimated to be $3.1*10^{-8}$ ft^{-1}.

10) A sensitivity test was also performed by splitting the computational layer 3 into two computational layers. With greater vertical resolution (four computational layers), the model took about the same amount of time to run and showed only minor changes in water elevations at observation well stations. Thus, the final ECM has the original three computational layers.

LS ECM

The numerical instabilities were reduced as much as possible in the LS ECM in order to improve the water budget error and the overall model performance.

Most of the instabilities in the MIKE 11 network were observed where the spacing between cross sections is much lower than the MIKE SHE grid cell size (750 ft). When MIKE SHE grid cells interact with the river network, it chooses the cross section location closer to the grid cell center to discharge the water from the drainage and overland components. If the cross sections are not spaced in one grid cell size or higher, MIKE 11 does not have storage assigned for that cross section and a spike in the stage may occur at that point and time while the water is not redistributed through the MIKE 11 branch. This numerical problem is solved by removing cross sections that are spaced too close to each other.

The maximum pumping rate in a few irrigation command areas (ICAs) was refined. This eliminated unrealistic oscillations in the GW head at those locations. The priority scheme in the irrigation module was changed from “none” to “equal shortage”, which is more appropriate. Moreover, the ICA code (dfs2) file was filtered in order to remove cells with natural land uses (codes from 7 to 20), which are unlikely irrigated in most of their extent.

Branches in some mining pits were removed to improve the model stability. Also, the hydraulic conductivities (K_h and K_v) in the conceptual mining pit lens were reduced from 1 to 0.1 m/s. All "bed only" leakance in MIKE SHE-MIKE 11 links were changed to "Aquifer + bed", which is more realistic.

For fine-tuning specific areas, the procedure followed to improve model performance varied from one site to another. In general, if there was a MIKE 11 branch involved, the model conceptualization of the area and the model parameters were revised. Typically the model conceptualization was changed and some corrections or adjustments were necessary for cross sectional data, flood codes, Manning roughness coefficients, leakage coefficients and conceptual weir elevations. The conductivity in the groundwater layers was typically adjusted in cases without any close MIKE 11 branches.

The option of “checking water levels before routing” for the case of the paved-area runoff coefficient was enabled to more accurately simulate gravity drainage systems.

Water Table Level in Mining Pits

In order to evaluate the LS ECM performance in mining pits, 62 values of water levels were extracted at different mining pits and lakes in the model domain area from the LIDAR data. Those points correspond to one day of year 2007, in accordance to the LIDAR flight date. The possible flight dates for those locations were June 18, 28 and 29; August 4, 5, and 6; and August 22, 23, and 24.

The mean water table differences between observed values and model predictions at those 62 locations in mining pits and lakes is presented in **Table 10** as computed from different model tests.

- A first intermediate test of the model (identified as LS ECM V1) overpredicts the water table levels on average in mining pits and lakes by 1.0 ft.
    - This step in the calibration process preceded the introduction of the refined topography or the distributed ET data.
- A second intermediate test of the LS ECM (marked with **) caused an improvement in the first result of 0.3 ft (mean difference of 0.7 ft).
    - This step uses the refined topographic map, revised flow ways conceptualized in MIKE 11 and drainage in some mining pits. Also uses the same station based ET as the ECM.
- A third intermediate test of the LS ECM (marked with *) caused an improvement of 0.4 ft compared to the second result (mean difference of 0.3 ft).
    - This step was modified with the new distributed reference ET (RET) data.

- The final version of the model (LS ECM) caused an improvement of 0.3 ft compared to the third step. This gives a net improvement of 1.0 ft, leaving a mean water table difference in mining pits of 0.0 ft. A zero mean difference does not mean that the water levels from the model are exact in all mining pits and lakes, but on average, the over- and under-predictions balance out.
    - In the final version, lake evaporation was modified to a value of RET + 8.0% to be applied in open water cells of the model.

This sequence reveals the importance of the different changes introduced in the model regarding the average water table levels predicted in mining pits, for which the inclusion of the distributed RET and a higher lake evaporation each had about the same impact as the changes caused by the inclusion of the new topography.

In the third test simulation of the model (LS ECM*), which differs from the early version (LS ECM**) due to adjustments during the recalibration, the average water table level differences in mining pits and lakes is less than 0.1 ft (using the absolute differences) for the two lake evaporation values considered of RET + 8.2% and RET + 5.3%, as shown in Table 10. In the final version of the model (LS ECM), obtained after further adjustments, the mean difference (D) is still below 0.1 ft, and the mean absolute difference (DA) is slightly lower than in previous versions.

Table 10. Mean water table differences in mining pits and lakes from several model runs.

Model	ET	LE – ET (% of ET)	D (ft)	DA (ft)
LS ECM V1	SET	0	-1.04	2.68
LS ECM**	SET	0	-0.7	---
	RET	0	-0.3	---
	RET	8.0	0.02	1.68
LS ECM *	RET	5.3	-0.06	1.67
	RET	8.2	0.01	1.66
LS ECM	RET	8.2	-0.07	1.65

Note: "D" stands for mean difference between LIDAR elevation and water level from the model and "DA" for the mean of the absolute differences. The early version of LS ECM is marked with "**" and the preliminary-report version of LS ECM is marked with an "*". See text for details.

Model Performance at Observation Stations

In order to evaluate the model, the performance metrics for groundwater and surface water observation stations were established. The statistical parameters and equations are shown in **Table 11**. Detailed tables and figures with the results at observation stations are presented in Appendix B for the ECM and in Appendix F for the LS ECM. In **Table 12**, the number of stations in three performance level ranges are summarized for different types of observation stations. These metrics are equivalent to those used in the SWFFS regional model for the groundwater stations, but the tolerance levels were reduced for the surface water

stations. A unique indicator of the performance level (PL) per observation station was calculated by averaging the levels of performance (1= high, 2= medium, or 3= low) obtained for each statistical parameter. For example, if the comparison of simulated surface water levels vs. the observed data in a given station results in a correlation value equal to or above 0.8, then the R parameter for this station has a score of 1. The average score for all the parameters in a given station is the PL value for that station.

Table 11. Statistical Parameters used for Calibration of the ECM.

Symbol	Name	Formula
ME	Mean error	$\overline{Obs_i - Calc_i} = \frac{1}{n}\sum_{i=1}^{n}\left(Obs_i - Calc_i\right)$
MAE	Mean Absolute Error	$\overline{\left\|Obs_i - Calc_i\right\|} = \frac{1}{n}\sum_{i=1}^{n}\left\|Obs_i - Calc_i\right\|$
RMSE	Root Mean Square Error	$\sqrt{\overline{\left(Obs_i - Calc_i\right)^2}} = \sqrt{\frac{1}{n}\sum_{i=1}^{n}\left(Obs_i - Calc_i\right)^2}$
R	Correlation Coefficient	$\frac{\sigma_{oc}^2}{\sigma_o \sigma_c}$ $\sigma_{oc}^2 = \overline{\left(Obs_i - \overline{Obs_i}\right)\left(Calc_i - \overline{Calc_i}\right)}$ $\sigma_o^2 = \overline{\left(Obs_i - \overline{Obs_i}\right)^2}\ \ \sigma_c^2 = \overline{\left(Calc_i - \overline{Calc_i}\right)^2}$

Table 12. Number of stations for different performance level ranges.

Type of observation point	Model ->	LS ECM		
	PL ->	1.0-1.5	1.6-2.4	2.5-3.0
	Total	Number of stations		
Mining Pits	62	22	24	16
Shallow Wells (Layer=1)	82	48	30	4
Intermediate Wells (Layer=2)	10	6	3	1
Deep Wells (Layer=3,4)	6	0	2	4
Surface Water	23	8	14	1

Note: "PL" stands for average performance level.

For stations where the model was underperforming, a visual inspection of the model results versus the observed data was conducted. This inspection was used to identify potential outliers in the observation files and other possible causes for the differences. Finally, the

average hydroperiod information received from KLECE for the DR/GR Area was utilized to perform a comparative evaluation of the hydroperiod predicted by the model within the DR/GR Area and to adjust the parameters to improve the model performance.

Water Table Elevation

Water table elevation maps predicted by the model are presented at two times of the year in **Figure 28** and **Figure 29**, corresponding to the end of the dry and wet season, respectively. Water table profiles along two transects in the DR/GR mining complex area (see **Figure 30**) are also presented in **Figure 31** to **Figure 34** at those times of the year for different models.

In the transect plots, the lower water table levels in mining pits and surrounding areas predicted from the LS ECM (identified as V2 in the figures) are noticeable with respect to the levels from the V1 model at the end of the dry and wet seasons. This is in accordance with the average 1-ft overprediction of the V1 model in the water table levels in mining pits that was removed through the calibration process (see Table 10). However, the differences in average water table levels between LE equal to 5.3% or 8.2% higher than RET are small, in correspondence with Table 10.

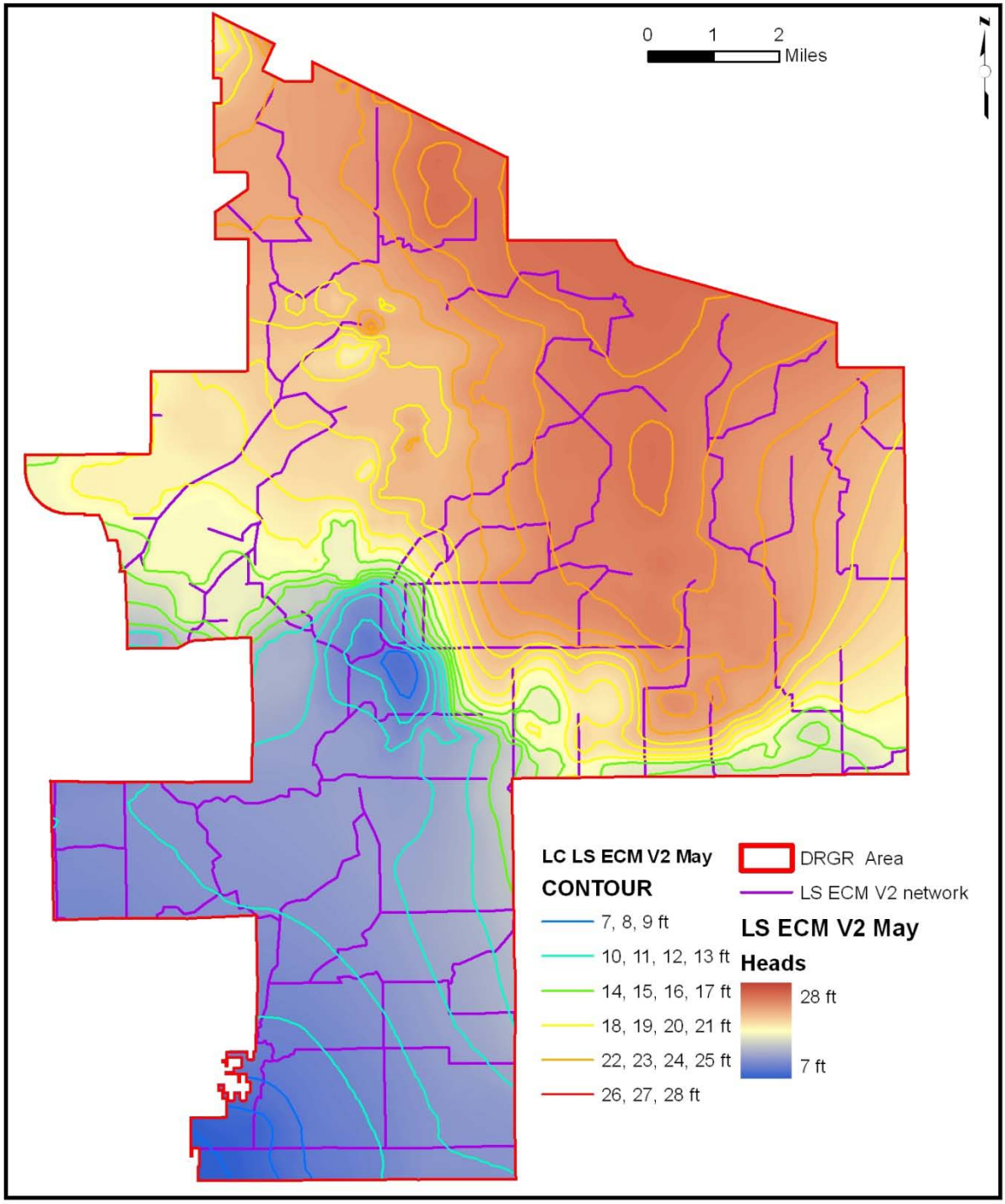

Figure 28. Average water table level map for the DR/GR Area at the end of the dry season as predicted by LS ECM.

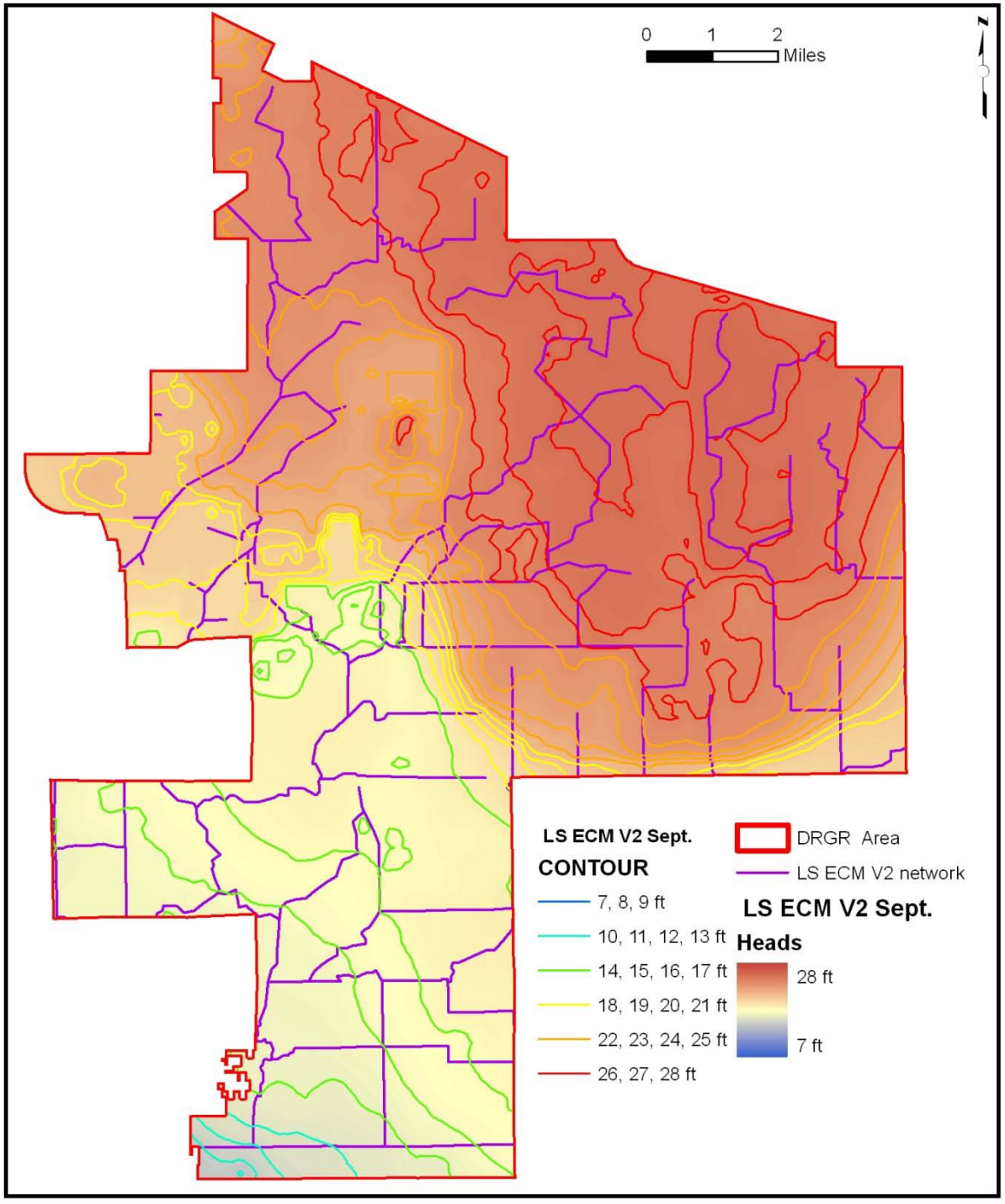

Figure 29. Average water table level map for the DR/GR Area at the end of the wet season as predicted by LS ECM.

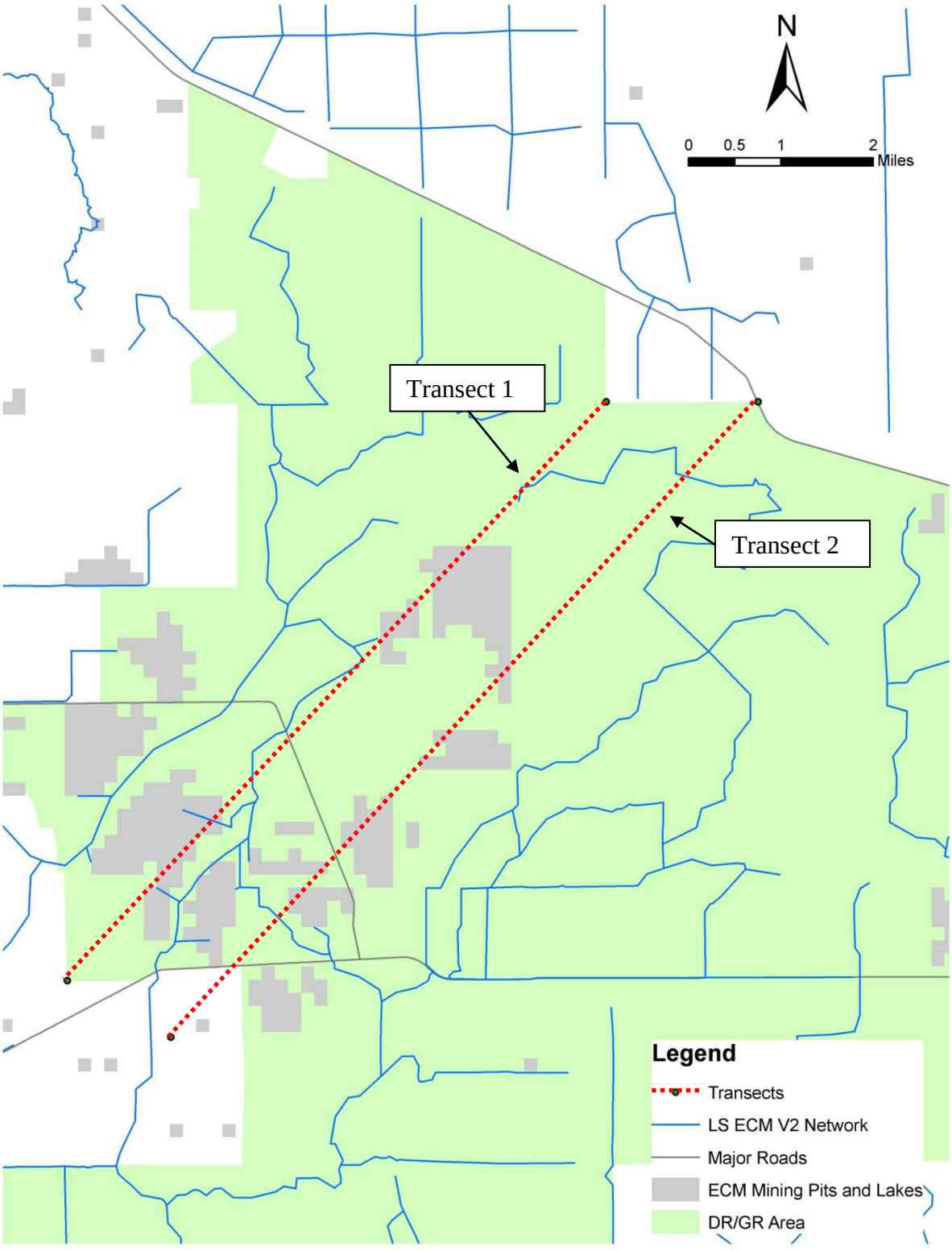

Figure 30. Transects through the mining pit complex area used to generate the water table level profiles presented from Figure 31 to Figure 34.

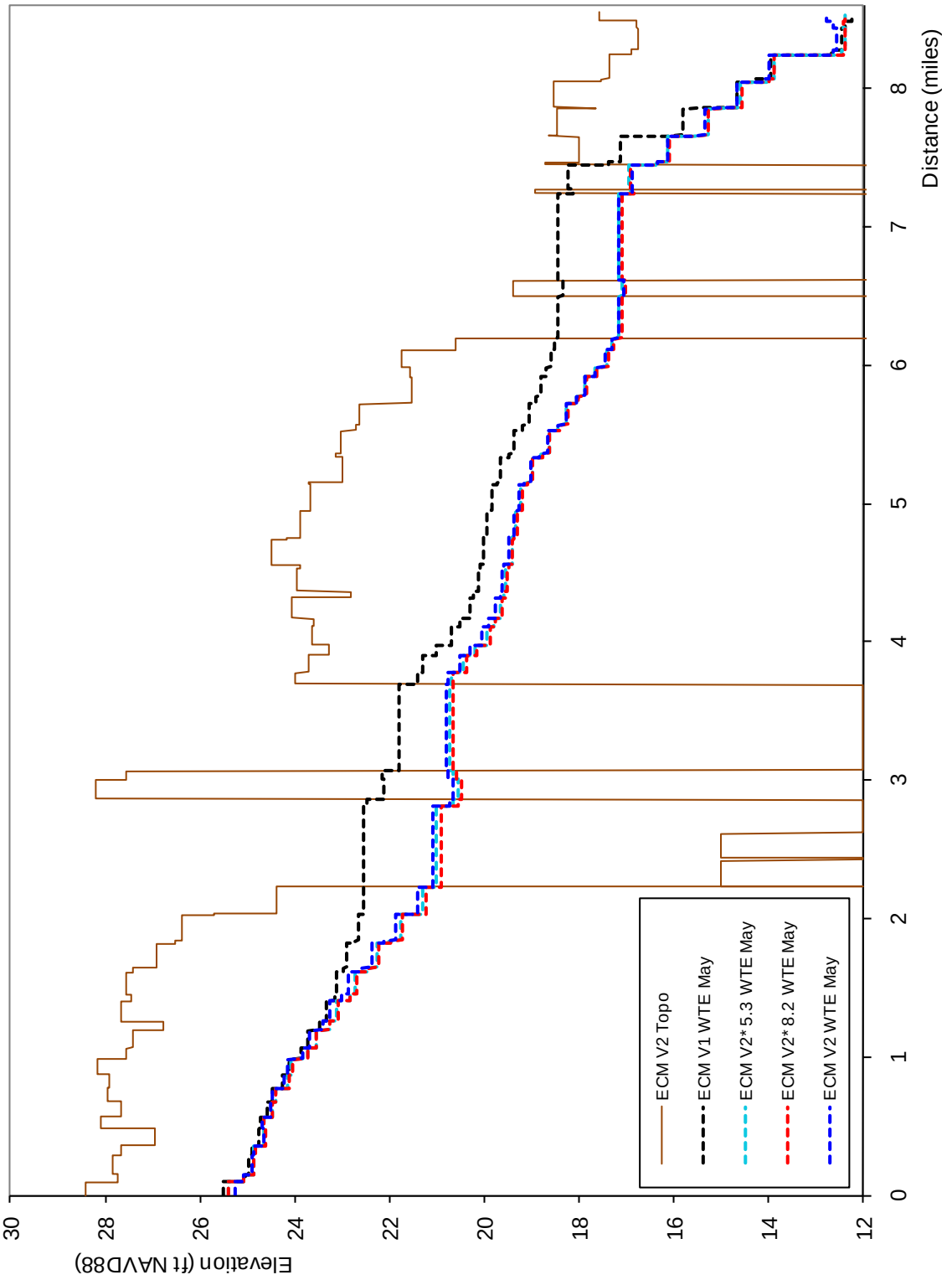

Figure 31. Water table level profile along Transect 1 presented in Figure 30 at the end of the dry season. The numbers 5.3 and 8.2 refer to the value in percent of LE - RET used.

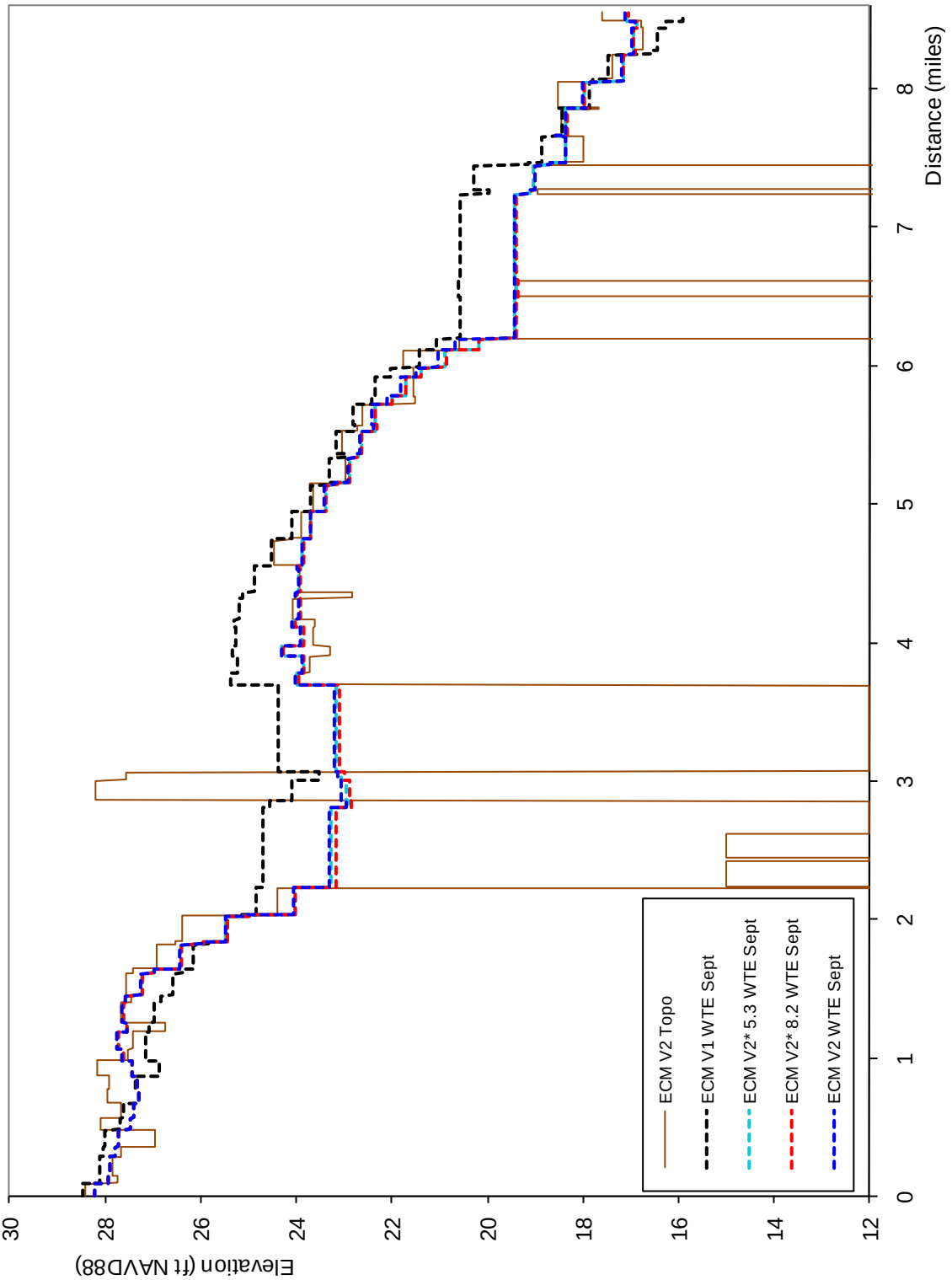

Figure 32. Water table level profile along Transect 1 presented in Figure 30 at the end of the wet season. The numbers 5.3 and 8.2 refer to the value in percent of LE - RET used.

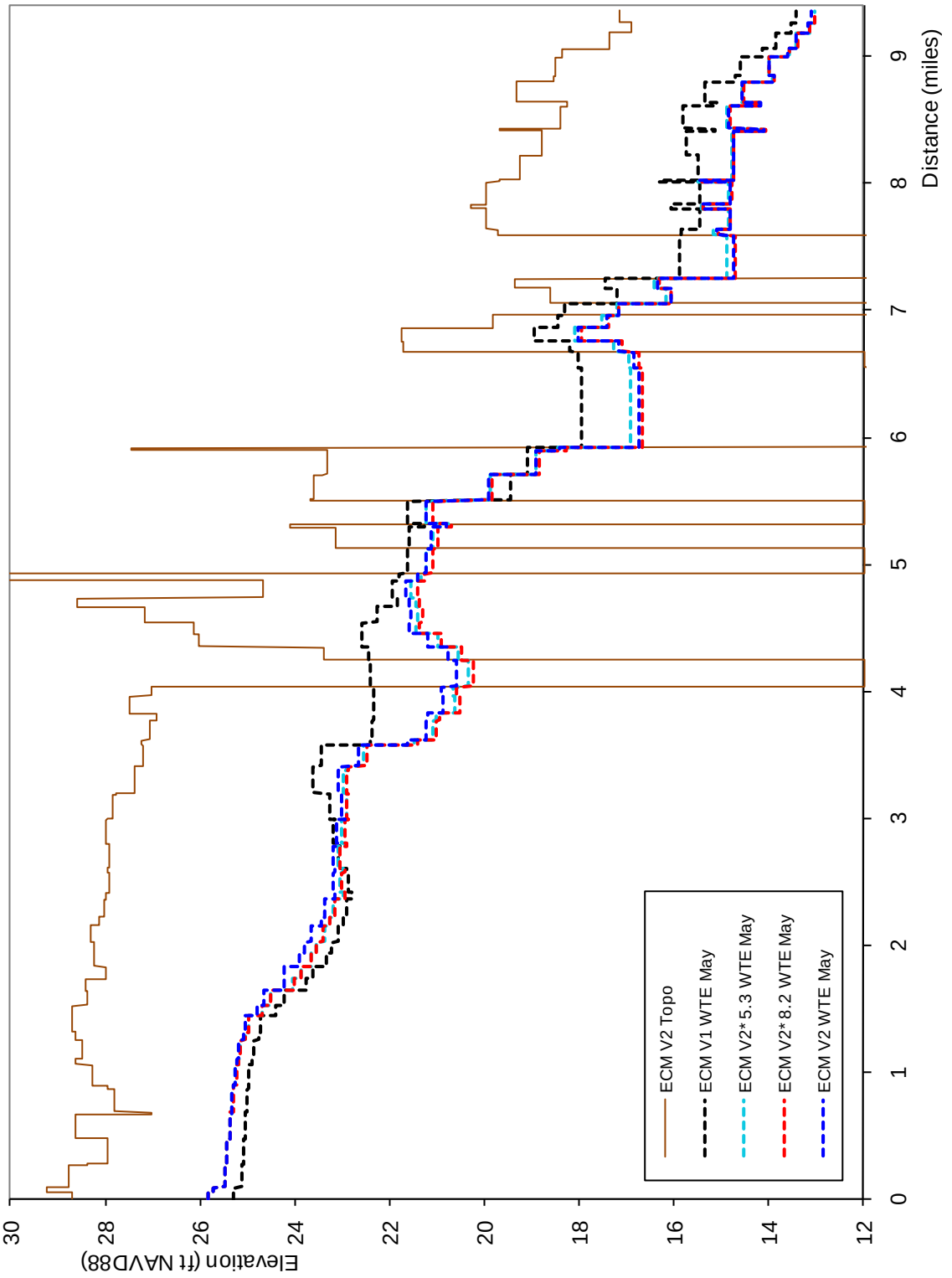

Figure 33. Water table level profile along Transect 2 presented in Figure 30 at the end of the dry season. The numbers 5.3 and 8.2 refer to the value in percent of LE - RET used.

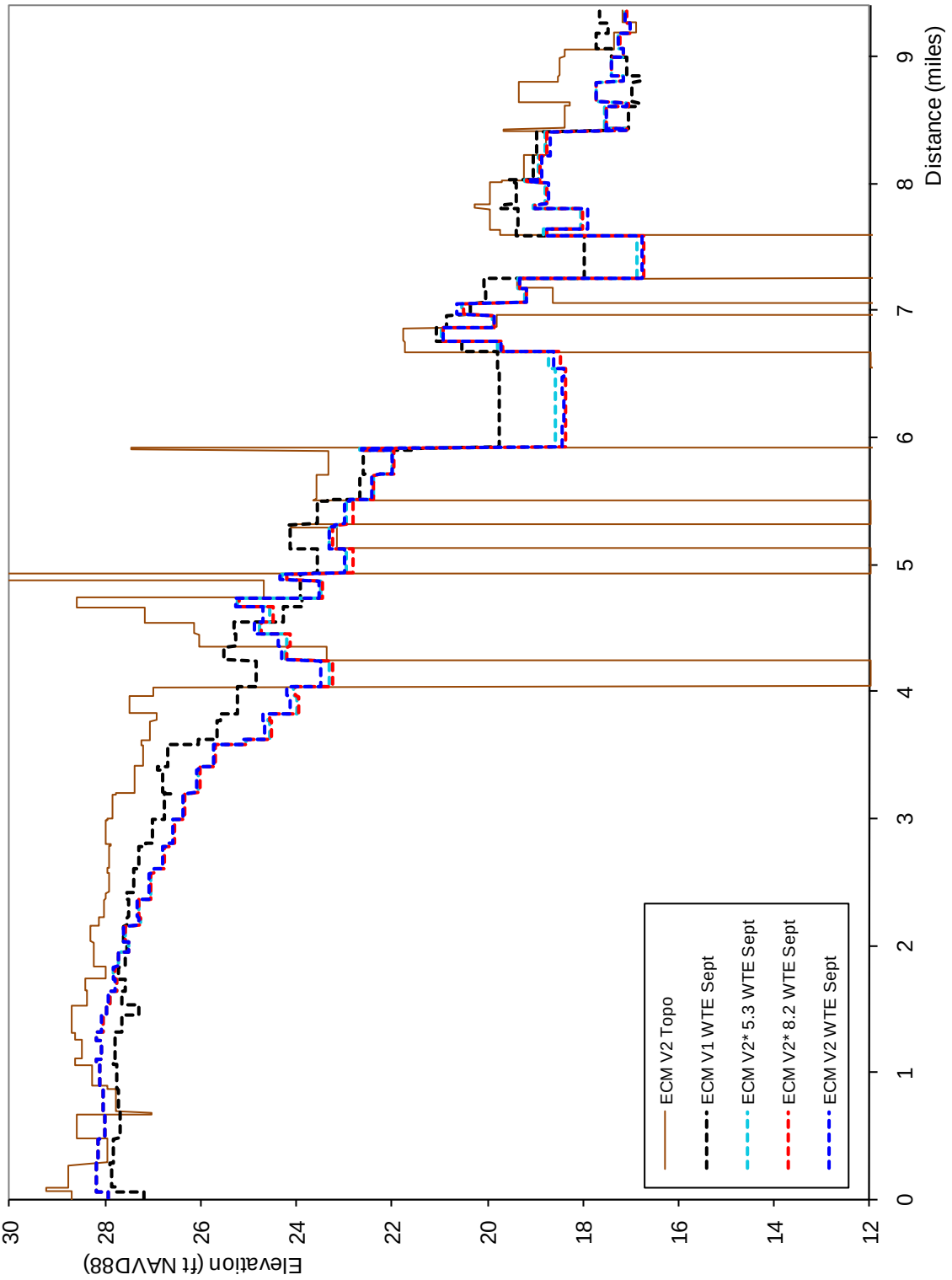

Figure 34. Water table level profile along Transect 2 presented in Figure 30 at the end of the wet season. The numbers 5.3 and 8.2 refer to the value in percent of LE - RET used.

Hydroperiod

The determination of the wetland hydroperiod has been an important indicator used in this study. A wetland hydroperiod has several definitions, but for this evaluation it is defined as the period during which water in the model is at least 1 mm above the topographic surface. The simulated wetland hydroperiod for the DR/GR Area was qualitatively compared with hydroperiod maps generated based on data created by KLECE [2008]. The model follows similar general trends but the comparison is limited due to the coarser resolution of the model in comparison to the map from KLECE data. The scaling limitations are evident when comparing the results of the local higher resolution model hydroperiod map to the KLECE map with higher resolution. Nevertheless, the hydroperiod output of the model together with the water table elevation and the water balance computation provide useful insight into the impact of the land use changes on wetland areas.

The hydroperiod data developed by KLECE is based on the vegetation communities, which have been mapped from GIS data and aerial photographs taken in 2007. This hydroperiod map was generated based on the estimated relationships among vegetation, hydroperiod, and water depth conditions. These are shown in the legend on **Figure 35**. According to KLECE, the estimated water depths and hydroperiods are typical ranges of conditions for unaltered wetland systems in southwest Florida (KLECE 2008). These relationships have not been compared with measured water level data, though. Thus, a quantitative or direct comparison between this hydroperiod map and the one produced by the model is not appropriate.

The hydroperiod map for the DR/GR Area and the corresponding map of mean water depths during the hydroperiod obtained from the model are presented in **Figure 36** and **Figure 37**, respectively. Other related maps can be found in Appendix H.

The hydroperiod map obtained from LS ECM* does not differ visibly when the lake evaporation changes from RET + 5.3 to RET + 8.2 (see maps in Appendix H). The same applies for the water depth maps during the hydroperiod. Thus, the hydroperiod maps do not show visible sensitivity to that change in lake evaporation.

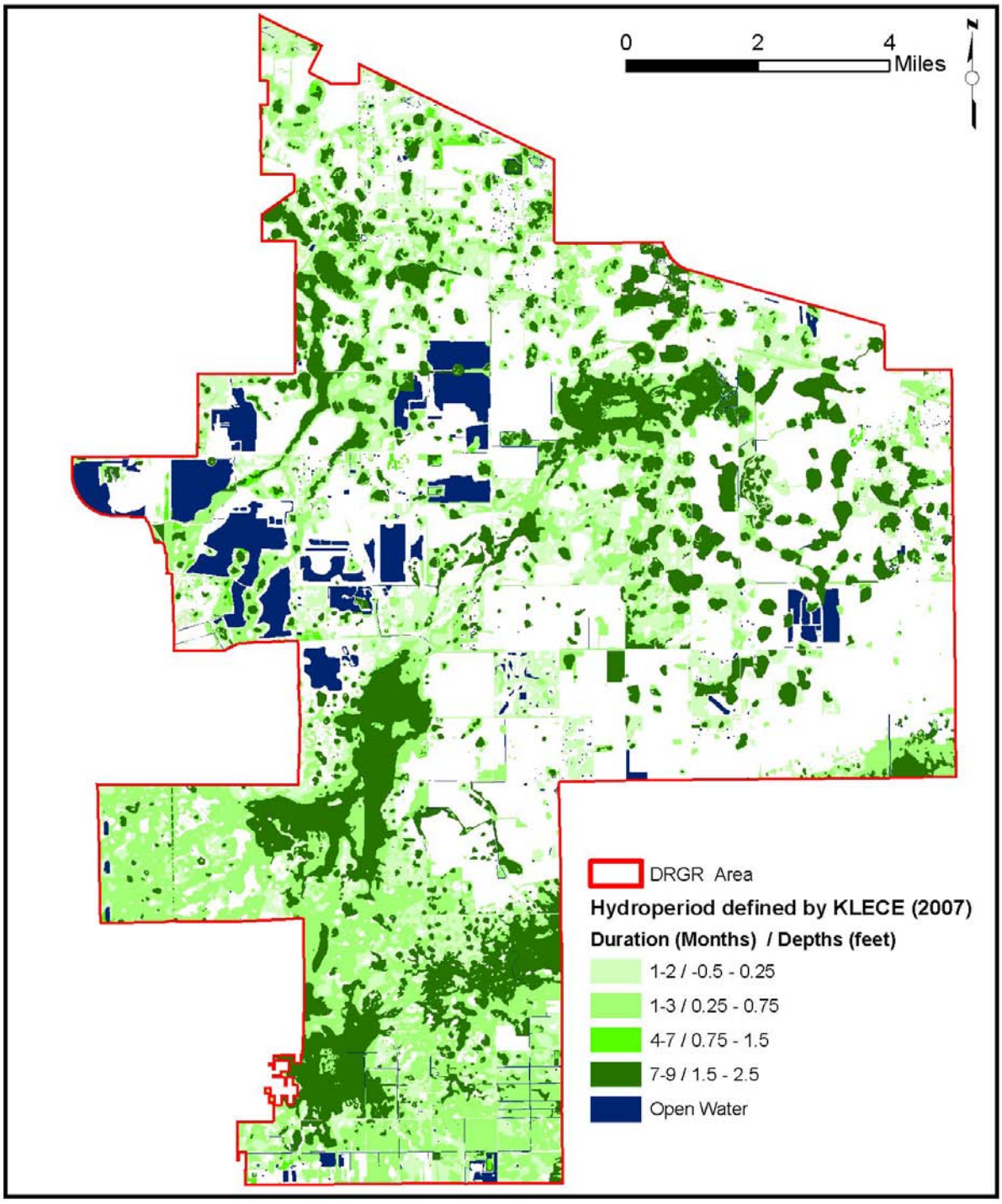

Figure 35. Hydroperiod map generated based on data created by KLECE from 2007 aerial photos.

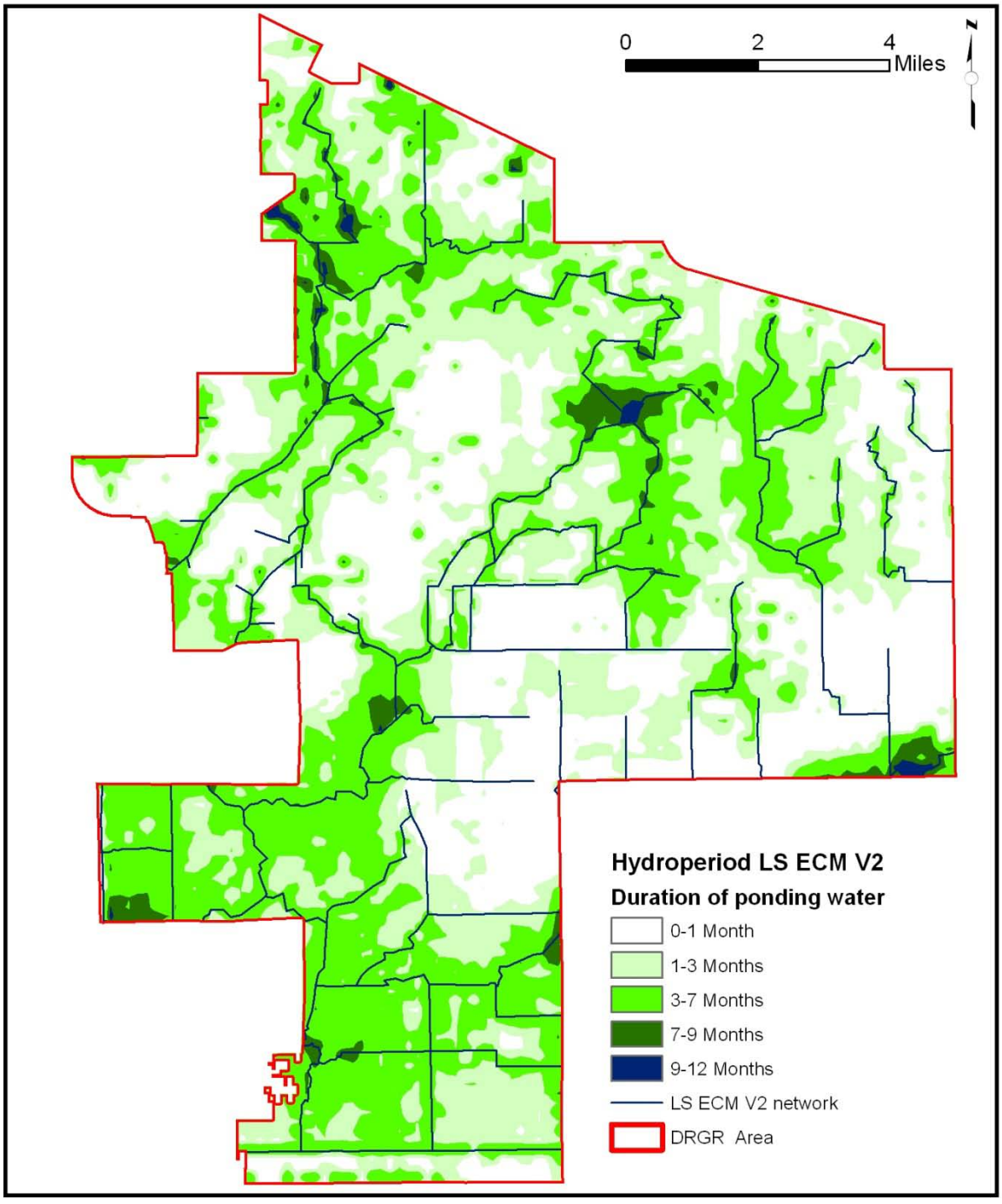

Figure 36. Hydroperiod map obtained from LS ECM.

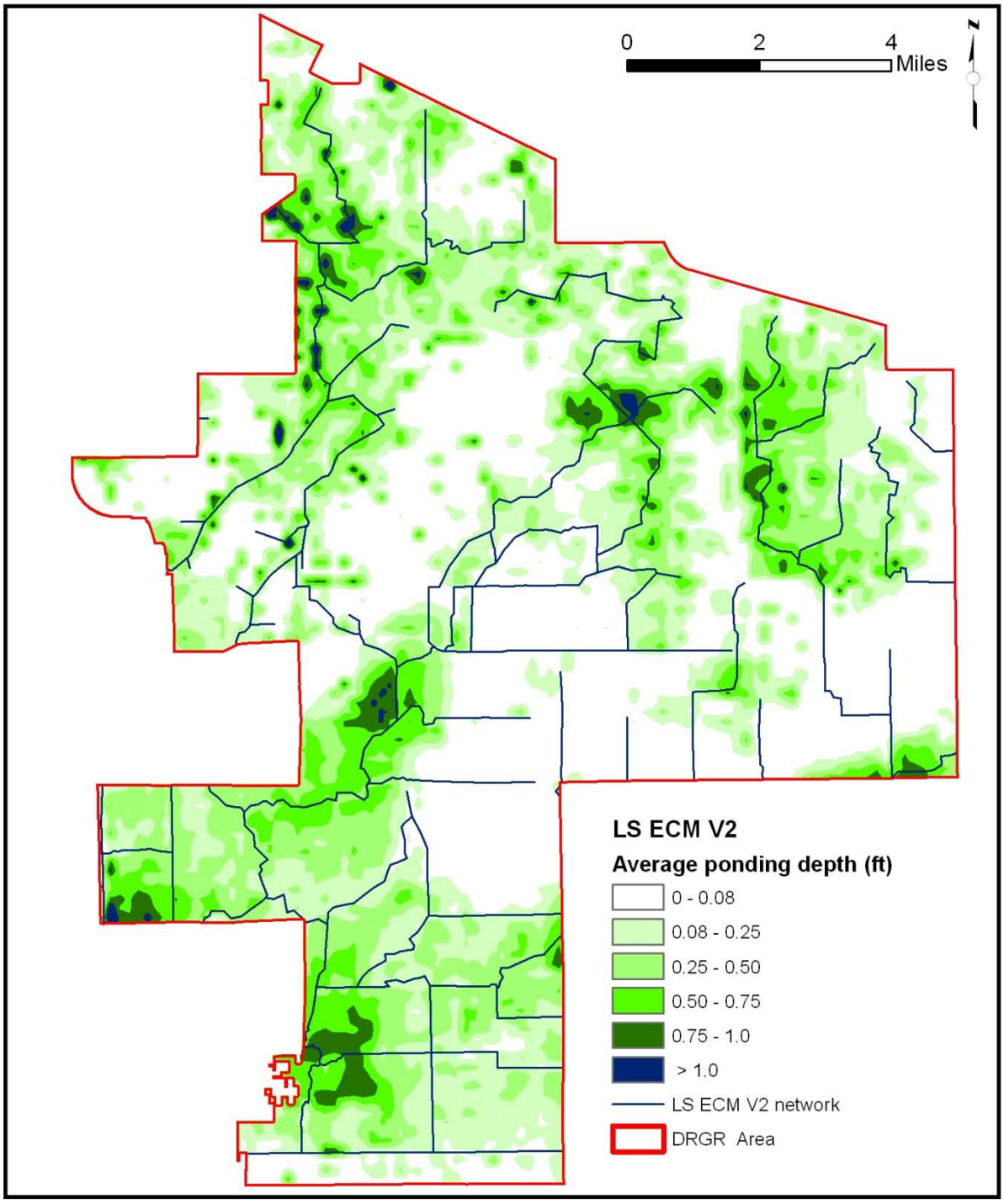

Figure 37. Hydroperiod water depth map obtained from LS ECM.

Water Budgets

A sketch of annual averaged water balance components obtained from the LS ECM in the entire DR/GR Area and in mining pits and shallow water bodies around the DR/GR area is presented in **Figure 38** and **Figure 39**, respectively. In **Table 13**, the water balance components from the final model and two intermediate models are displayed for comparison of the impact the lake evaporation has on the overall water budgets. All those water balance depth rates reported are annual averaged values for the 5-year period from 2002 to 2006.

Naturally, the increased ET rates in the open water bodies decreases the net rainfall (rainfall minus ET) in these areas. In fact, a lake evaporation of RET + 8.2% produces a net rainfall of zero inches per year in mining pits and lakes. Furthermore, the inclusion of a drainage system in some mining pits causes a net surface water outflow from mining pits and lakes in the model. As a result, the model predicts a negative groundwater outflow from the mining pits and open water bodies.

The overall water budget in the DR/GR area indicates that the higher ET rate and other changes made to the model causes a reduced boundary outflow through the groundwater, overland layers, and also through the rivers.

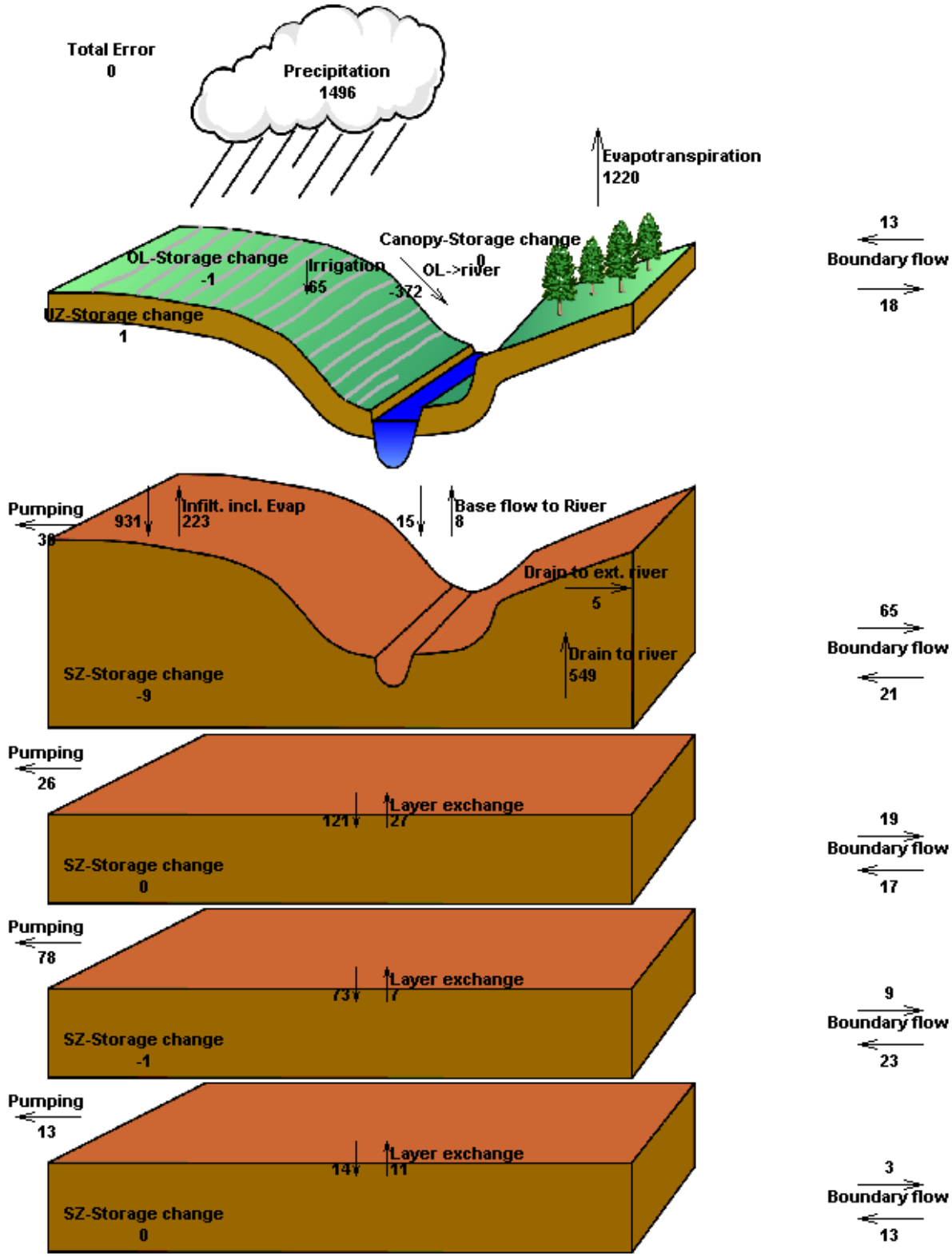

Figure 38. Annual averaged water balance components in mm/yr for the entire DR/GR Area as predicted by the LS ECM.

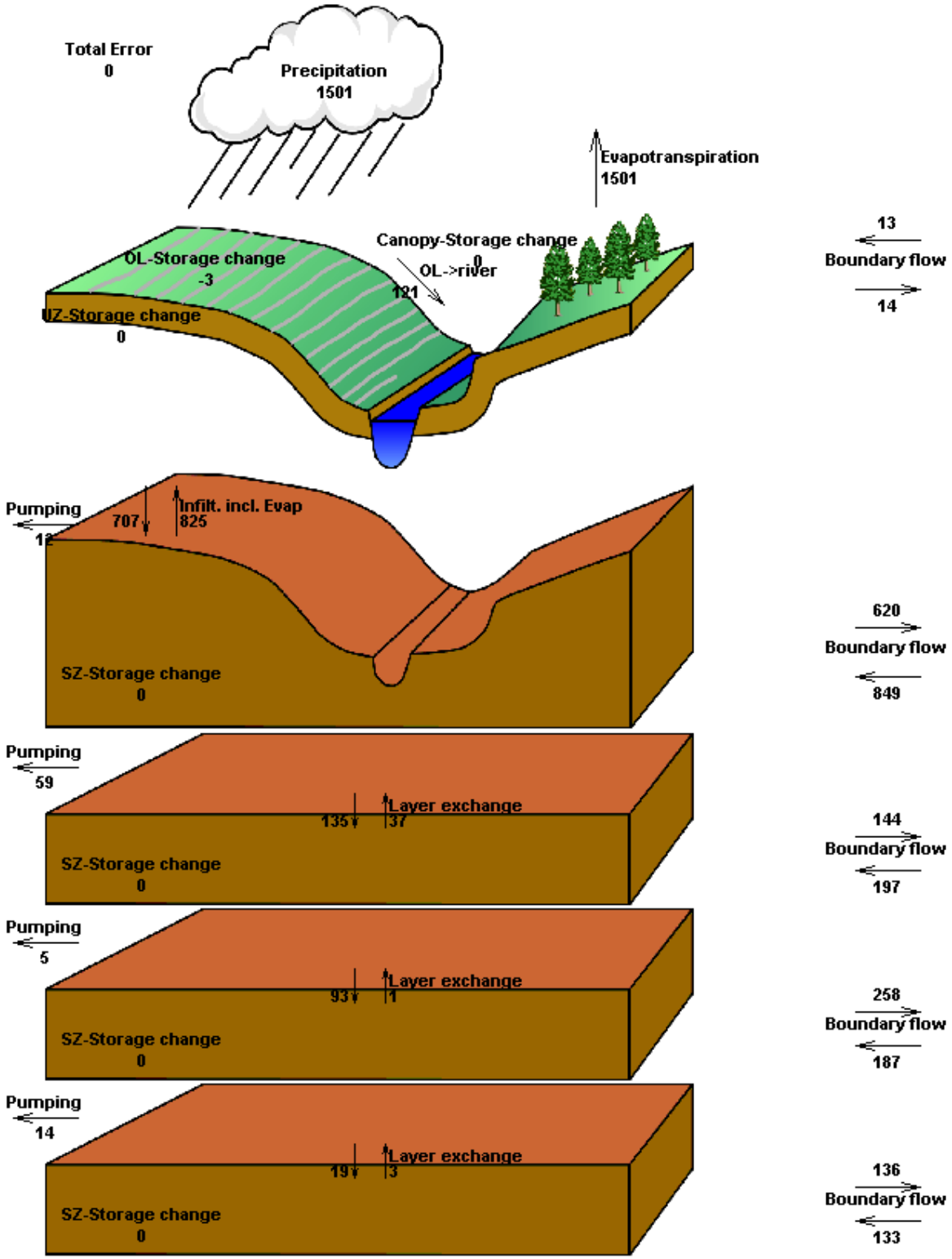

Figure 39. Annual averaged water balance components in mm/yr for the mining pits and other shallow water bodies around the DR/GR Area as predicted by the LS ECM.

Table 13. Annual average depth rates of the water balance components from the different versions of LS ECM, different ET data and in two different areas: in the entire DR/GR and in the Mining Pits and shallow water bodies in and around the DR/GR Area.

	Area	DR/GR			Mining Pits		
	LS ECM version	ECM*	ECM*	ECM	ECM*	ECM*	ECM
	ET	RET	RET	RET	RET	RET	RET
Depth rates (inches/year)	**LE - ET (% of ET)**	**5.3**	**8.2**	**8.2**	**5.3**	**8.2**	**8.2**
Rainfall		58.9	58.9	58.9	59.1	59.1	59.1
ET		48.1	48.1	48.0	57.5	59.1	59.1
Rainfall - ET (A)		**10.8**	**10.7**	**10.9**	**1.6**	**0.0**	**0.0**
OL storage change		0.0	0.0	0.0	-0.2	-0.2	-0.1
UZ Storage change		0.0	0.0	0.0	0.0	0.0	0.0
Total SZ Storage change (BSZ)		-0.4	-0.4	-0.4	0.0	0.0	0.0
Total storage (B)		**-0.4**	**-0.4**	**-0.4**	**-0.2**	**-0.2**	**-0.2**
Net OL Boundary outflow (COL)		0.1	0.1	0.2	0.0	0.0	0.0
Drain to Boundary (CDR)		0.0	0.0	0.0	0.0	0.0	0.0
Net SZ Boundary outflow from SZ1		1.7	1.7	1.7	-8.0	-9.0	-9.0
Net SZ Boundary outflow from SZ2		0.0	0.0	0.1	-2.1	-2.2	-2.1
Net SZ Boundary outflow from SZ3		-0.6	-0.6	-0.5	3.0	2.9	2.8
Net SZ Boundary outflow from SZ4		-0.4	-0.4	-0.4	0.2	0.1	0.1
Net SZ Boundary outflow from all SZ (CSZ)		0.8	0.8	0.9	-7.0	-8.2	-8.2
Total Boundary outflow (C)		**0.9**	**0.9**	**1.1**	**-7.0**	**-8.1**	**-8.2**
Pumping from SZ1		1.5	1.5	1.2	0.6	0.6	0.5
Pumping from SZ2		1.1	1.1	1.0	2.5	2.5	2.3
Pumping from SZ3		3.3	3.3	3.1	0.2	0.2	0.2
Pumping from SZ4		0.5	0.5	0.5	0.6	0.6	0.6
Pumping from all SZ		6.4	6.4	5.8	3.8	3.8	3.6
Irrigation		3.2	3.2	2.5	0.0	0.0	0.0
Pumping-Irrigation (D)		**3.2**	**3.2**	**3.2**	**3.8**	**3.8**	**3.6**
Infiltration from OL to SZ1		27.5	27.4	27.9	-3.2	-4.4	-4.7
Infiltration from SZ1 to SZ2		3.9	3.9	3.7	4.2	4.0	3.9
Infiltration from SZ2 to SZ3		2.8	2.8	2.6	3.8	3.8	3.6
Infiltration from SZ3 to SZ4		0.1	0.1	0.1	0.7	0.7	0.7
OL->river		-13.7	-13.6	-14.7	4.9	4.5	4.8
Drain to river		20.7	20.6	21.6	0.0	0.0	0.0
Drain to ext. river		0.2	0.2	0.2	0.0	0.0	0.0
Base flow to River		-0.2	-0.2	-0.3	0.0	0.0	0.0
Total flow to river (E)		**7.0**	**7.0**	**6.9**	**4.9**	**4.5**	**4.8**
Error (A-B-C-D-E)		0.0	0.0	0.0	0.0	0.0	0.0
Boundary surface outflow (runoff)	COL+CDR+E	7.2	7.1	7.1	5.0	4.6	4.8
	COL+CDR	---	---	---	---	---	---
Net groundwater recharge	A-(B-BSZ)-(C-CSZ)-E= BSZ+CSZ+D	3.6	3.6	3.7	-3.2	-4.4	-4.7
	A= B+C+D+E	---	---	---	---	---	---

Note: the preliminary version of LS ECM is marked with an "*".

Surface Water Flow

Figure 40 shows the annual average flow rate in the MIKE 11 network as predicted with the LS ECM from year 2002 to 2006. Primary flow ways are the ones having higher averaged flow rates. The sudden changes in color in the branches primarily indicate the interaction with the overland component of MIKE SHE, i.e., locations where water is flowing between the rivers and the flood plains. The annual average flow map suggests that the MIKE 11 network generated following incorporation of the high resolution LIDAR data into the LS ECM more accurately represents the main flow ways in the DR/GR Area compared to its performance prior to the reanalysis of the flow ways. Further refinement in the network can be conducted by removing branches with negligible flow (that are not visible in Figure 40) and by checking the path and cross section geometry in locations with high interaction with overland flow.

A closer look to the annual average flow rate through the conceptual weirs around mining pits (that were introduced to represent the drainage system) is presented in **Figure 41**. Single sided arrows are used to represent the net flow direction and double sided arrows are used where there are important flows in both directions. The instantaneous flow rates at some of those weirs are plotted in **Figure 42**. According to the model, mining pits with conceptual weirs at locations D and G may serve as reservoirs, collecting water during the rainy season and releasing it early in the dry season. Mining pits with conceptual weirs at locations E-F and I-J may serve to route surface water in the southwest direction. A positive or negative net annual flow rate into a mining pit may indicate whether the specific mining pit is contributing to the groundwater recharge or discharge, respectively. The drainage system around the mining pits is based on LIDAR data elevations and other model assumptions. Observation data to compare and validate those model results were not available at that time.

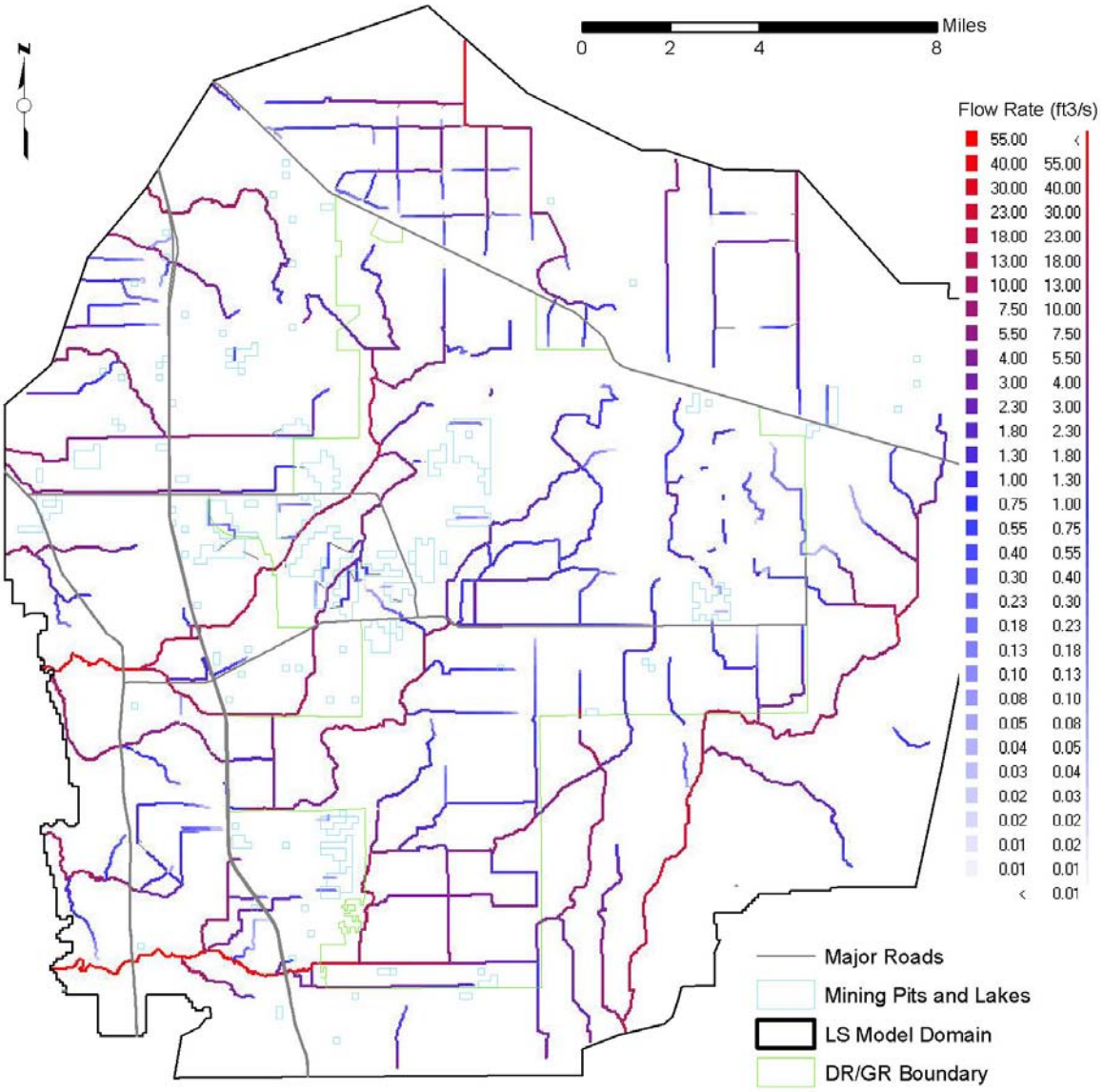

Figure 40. Annual averaged flow rates obtained at the river network from the LS ECM**.**

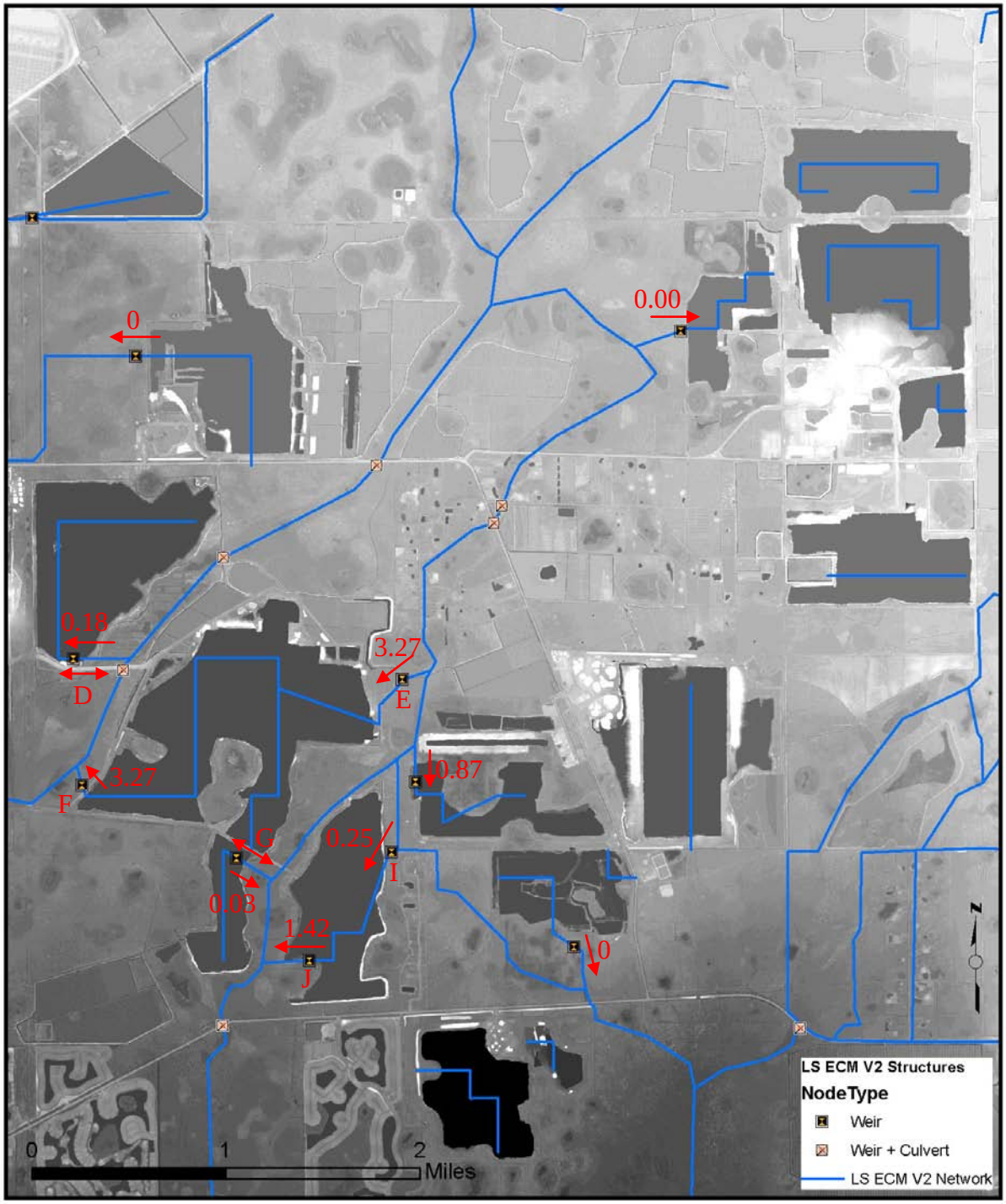

Figure 41. Annual averaged flow rates (in ft^3/s) in the drainage system around mining pits as obtained from the LS ECM.

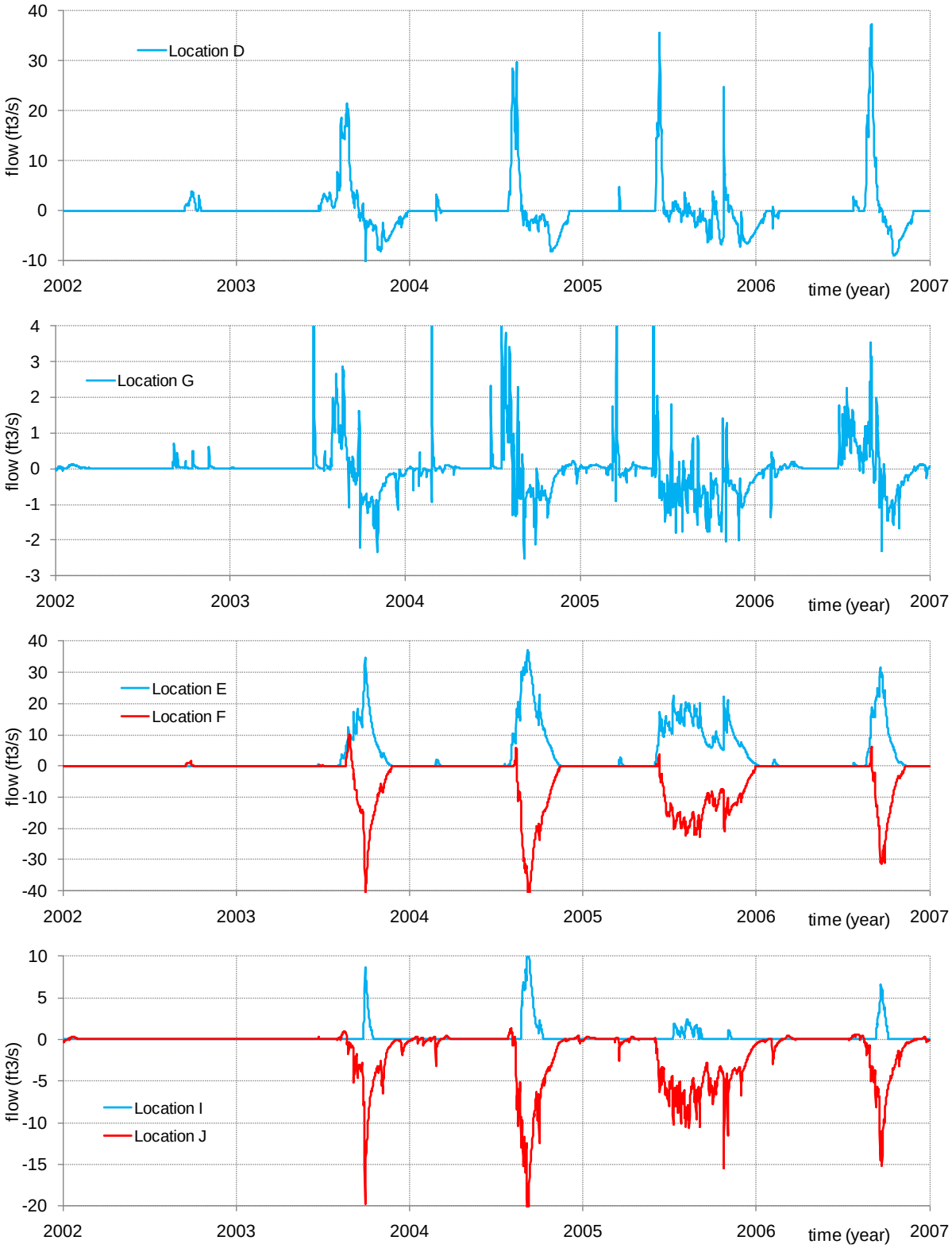

Figure 42. Flow rates at some conceptual weirs around mining pits presented on Figure 41.
Note: solid blue and red lines are used when positive flow is toward and away from the mine, respectively**.**

Land Use Scenarios

In order to evaluate the hydrological effects of land use changes in the DR/GR Area, four Future Conditions Models (FCMs) were developed. The results of these models were analyzed by using relative measures, such as differences in hydroperiod, water table elevations, and overall water budget.

Development of Future Land Use Alternatives

The future land use scenarios consist of four alternatives in the DR/GR Area provided by Lee County (see land use maps in Appendix D). The land use changes are of three types: creation of urban areas, expansion or creation of mining pits and restoration of agricultural lands into wetlands. Land use alternative 1 (FCM1) is conceptually similar to Scenario 1 in "Prospects for Southeast Lee County" [Dover, Kohl & Partners, July 2008]. Mining would be limited to already-approved mining pits plus some new pits north of Alico Road near the airport (but fewer pits than in Scenario 1). A broad westerly flow way to Corkscrew Swamp would be restored southward from the Imperial Marsh. Land use alternative 2 (FCM2) is conceptually similar to Scenario 2 in the Dover Kohl report. Mining would be limited to already-approved pits plus a major expansion to the Green Meadows Mine. A broad flow way to Corkscrew Swamp would be restored southward from the east end of Corkscrew Road in Lee County. Land use alternative 3 (FCM3) is conceptually similar to Scenario 3 in the Dover Kohl report. Mining would be limited to already-approved pits plus proposed new pits that were in the application process in September 2007, including pits along Corkscrew Road east of the Flint Pen Strand. Both flow ways to Corkscrew Swamp would be restored to whatever extent is still possible after significant portions of each were mined. Land use alternative 4 (FCM4) is conceptually similar to an alternative scenario that emerged favorably during public meetings after release of the Dover Kohl report. Mining would be limited to already-approved pits plus a moderate expansion to the Green Meadows Mine. Both flow ways to Corkscrew Swamp would be restored in full. The extent of the restored areas in all scenarios is less than originally proposed in the Dover Kohl report.

The new urban areas added in the future conditions land use map were exactly the same in all four alternatives. The increase of new mining areas from smallest mining area to largest mining area is: FCM1, FCM4, FCM2, and FCM3. The mining area in FCM3 is nearly double the amount of mining area in FCM1. The amount of mining area in FCM2 and FCM4 are approximately the same, and these scenarios fall in between FCM3 and FCM1, with respect to mined area. The total amount of newly restored areas increases monotonically from FCM1 to FCM4. FCM3 is a unique case in that its restored areas are imbedded with mining pits. Figures and tables in Appendix D show more details of the land use changes for all scenarios.

All land use based parameters in the model (e.g., overland roughness Manning's coefficient, detention storage, paved runoff fractions, drainage depths and drainage time constants) were modified to correspond to the new land use maps, but the relationship between land use type and parameters remained consistent with the ECM. The same meteorological and boundary conditions data utilized in the ECM were used in the four FCMs. The irrigation setup

in the future conditions model was modified to reflect future land use changes. For example, irrigation areas were removed in areas where the land use was converted from urban or agricultural to mining or wetland areas. For new urban areas, irrigation was added in those close to the northern DRGR boundary. The monthly groundwater withdrawal rates of the most recent year of available groundwater withdrawal data were repeated for every year in the FCM simulation period (2002-2007). In some cases, the 2007 withdrawal rates were used if available, but in others the 2006 rates were used. The same groundwater withdrawal rates for public water supply were used for the four future conditions scenarios. The domestic self supply rates vary according to land use changes.

Initial Conditions

Special effort was conducted to obtain initial conditions that are representative of "average" or "steady state" conditions in the LS FCMs, as in the final version of the LS ECM. The SFWMD technical staff recommends a warming period of several months in the model (including an entire rainy season) in order to make the model results independent of the initial condition assumed. However, in the DR/GR model, there are two slow processes that need more than one year in order to remove the long term "drift" caused by assuming inaccurate initial conditions. They are the head in the deepest layer (sandstone aquifer) and the water level in mining pits.

Three to five iterations (running the model for three years and taking the results from September 1, 2004 as initial conditions for the next run) were necessary to assure that the differences in water elevation in mining pits between iterations is less than 10 cm.

Assuming "average" or "steady state" initial conditions in the FCMs means that the model is evaluating the water resources at some time long after the land use changes. In other words, the period of time during which those land use changes are being made are not simulated in the model.

Results

The results shown in this section demonstrate the potential effect of land use alternatives on the water resources of the DR/GR Area. Water table levels at specific locations (where changes in land use occur) were plotted for the different scenarios to compare the water table level changes throughout the five year simulation period. Averaged water table elevation maps were created for all land use alternatives for two times of the year: at the end of the dry season (end of May) and at the end of the wet season (end of September). Hydroperiod maps and maps of the mean water depth during the hydroperiod were also produced for all scenarios. Water table level and hydroperiod map differences between the FCMs and the ECM are also presented.

The water budget for the entire DR/GR Area was calculated to determine what hydrologic components were affected by the different alternatives. Finally, changes in surface water flow were calculated at specific locations for each scenario.

Water Table Plots

Figure 43 to **Figure 46** illustrate the specific locations where the changes in water table elevation were compared for all land use alternatives throughout the 5-year simulation period. The water table elevation plots are shown in **Figure 47** to **Figure 69**. The following results arise from those comparative plots:

- In all the locations converted to mining pits (M2, M6, M7, M8, M12, and M15), the seasonal amplitude of the water table oscillation is reduced, which is an expected consequence of increased open-water storage in mining pits.
- The model results in locations M1, M2 and M3 (see **Figure 70**) predict that the mine is acting like a groundwater reservoir, i.e., releasing water (collected during the rainy season) into the aquifers during the dry season. As a result, the seasonal amplitude of the water table oscillation around the mine pit is reduced, and particularly, the water table level during the dry season is higher. This effect is an expected consequence of the higher open-water storage than in the neighboring porous media. In the Water Budget section, further analysis of this proposed mine is conducted by computing the water balance components.
- Locations M4, M5, M6 and M7 are upstream of a mining pit complex in the DR/GR Area, and locations M8, M9 and M10 are downstream. As predicted by the model, larger and more closely spaced mining pits in the FCM create a larger flattening effect over the regional water table gradient. Specifically, the dry-season water table level decreases up gradient and increases down gradient. This effect was also observed on a smaller scale around single mining pits in locations with steeper slopes at locations M11 and M13. The areal extent of zones with lower and higher water table levels can be seen in the maps presented in the following section.
- In two of the three locations converted to wetlands (W2 and W3), the dry-season water table elevation increases. In the case of location W3, that increase is higher when it is close to new mining pits (in FCM3).
- Most of the new urban locations (U1, U2, and U3) showed a slight decrease in the wet-season water table elevation, which is likely a consequence of the new urban drainage. An increase in the dry-season water table elevation is observed in most of the new urban locations (U1, U3, and U4), which is likely related to a reduction in the ET losses (see more details in the water budget section).

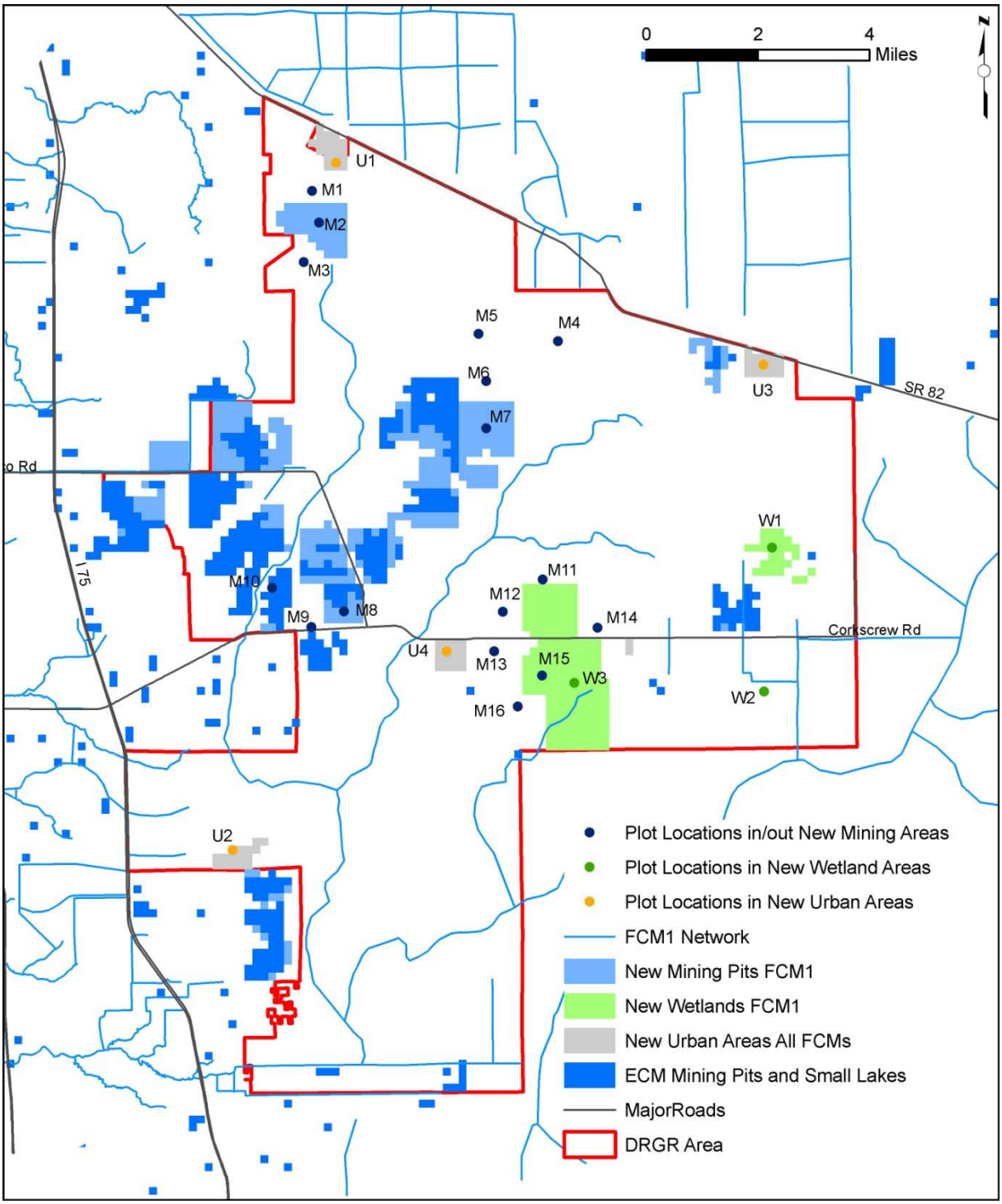

Figure 43. Land use changes in the Future Conditions Model 1 and locations of water table comparison plots.

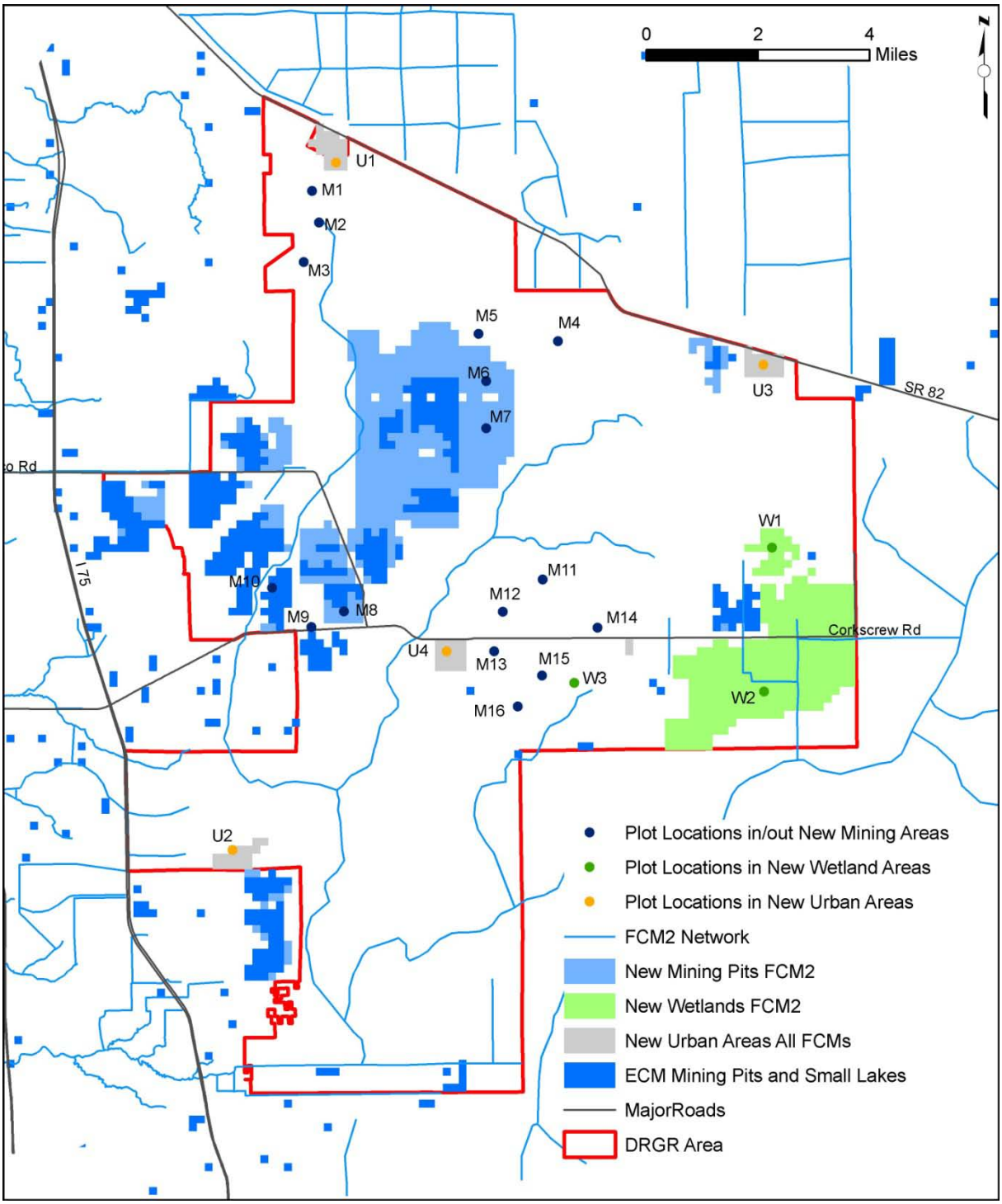

Figure 44. Land use changes in the Future Conditions Model 2 and locations of water table comparison plots.

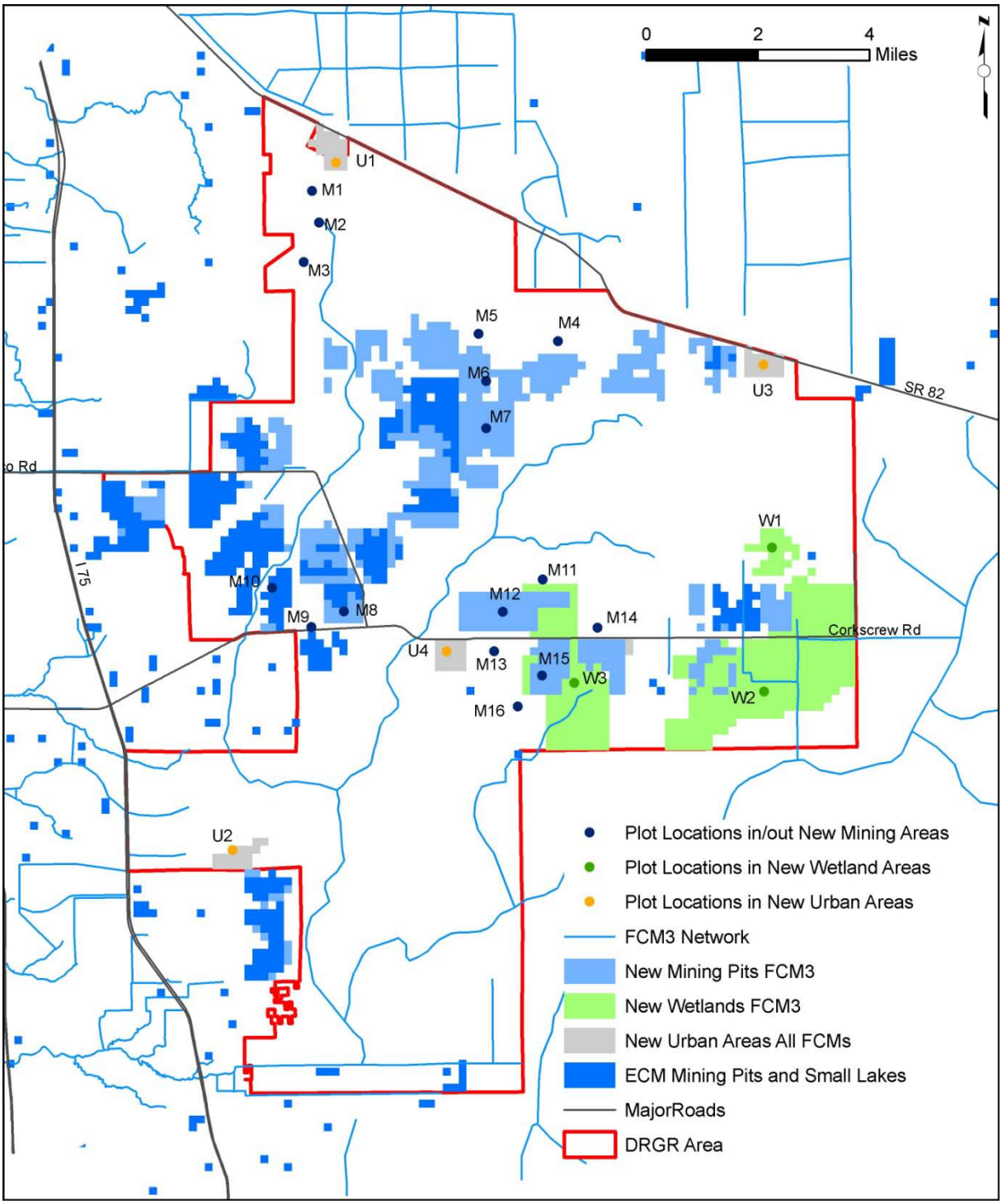

Figure 45. Land use changes in the Future Conditions Model 3 and locations of water table comparison plots.